

# ReST-KV: Robust KV Cache Eviction with Layer-wise Output Reconstruction and Spatial-Temporal Smoothing

Anonymous ACL submission

## Abstract

Large language models (LLMs) face growing challenges in efficient generative inference due to the increasing memory demands of Key-Value (KV) caches, especially for long sequences. Existing eviction methods typically retain KV pairs with high attention weights but overlook the impact of attention redistribution caused by token removal, as well as the spatial-temporal dynamics in KV selection. In this paper, we propose **ReST-KV**, a robust KV eviction method that combines layer-wise output Reconstruction and Spatial-Temporal smoothing to provide a more comprehensive perspective for the KV cache eviction task. Specifically, ReST-KV formulates KV cache eviction as an optimization problem that minimizes output discrepancies through efficient layer-wise reconstruction. By directly modeling how each token’s removal affects the model output, our method naturally captures attention redistribution effects, going beyond simplistic reliance on raw attention weights. To further enhance robustness, we design exponential moving average smoothing to handle temporal variations and an adaptive window-based mechanism to capture spatial patterns. Experiments show that ReST-KV improves average accuracy by up to 2.58% over state-of-the-art baselines on Long-Bench, consistently outperforms existing methods on RULER, Needle-in-a-Haystack, and InfiniteBench, and achieves a  $10\times$  reduction in decoding latency at 128k context length. Code is included in the supplementary material and will be released soon.

## 1 Introduction

Large language models (LLMs) (Achiam et al., 2023; Anthropic, 2023; Dubey et al., 2024; MistralAI, 2023) have significantly advanced natural language processing (NLP). These models have enabled breakthroughs in various tasks, such as document summarization (Zhang et al., 2024a), multi-turn dialogues (Du et al., 2021), retrieval aug-

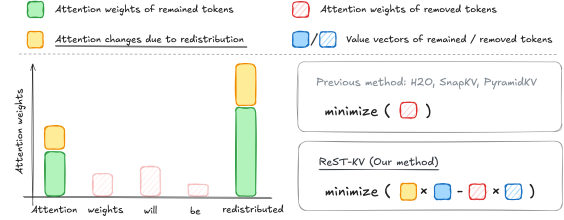


Figure 1: Comparison between ReST-KV and existing methods. Unlike prior approaches that overlook attention redistribution, ReST-KV considers its impact to improve KV retention under limited cache.

mentation (Yao et al., 2022), and code generation (Roziere et al., 2023). Recent models like GPT-4 (Achiam et al., 2023), Claude 3.5 (Anthropic, 2023), and Llama-3.1 (Dubey et al., 2024) have extended their context lengths beyond 128K tokens, allowing for long-context applications. However, as context length increases, the memory required to store KV cache grows rapidly, potentially reaching hundreds of gigabytes when handling longer sequences. Thus, optimizing KV cache during inference, without retraining, is crucial for improving both efficiency and scalability.

KV cache eviction, which identifies and removes less important KV pairs, is a promising approach to reduce memory consumption and enhance computational efficiency (Li et al., 2024a). Current methods typically rely on fixed attention patterns (Han et al., 2024; Ge et al., 2023) or use statistical information from attention weights (Zhang et al., 2023; Li et al., 2024b; Cai et al., 2024) to estimate the importance of KV pairs. However, as shown in Figure 1, these approaches focus solely on retaining query-key pairs with high similarity scores, while ignoring the attention redistribution effects caused by removing certain pairs. This redistribution can alter the overall attention landscape, leading to sub-optimal retention decisions and degraded performance, especially under tight cache constraints.

In this paper, we propose ReST-KV, a robust KV cache eviction method that accounts for the

effects of attention redistribution and the spatial-temporal dynamics in KV selection. We revisit the KV cache eviction problem and reformulate it as preserving the attention output at each layer under fixed memory constraints. Specifically, we measure the reconstruction loss caused by removing each individual KV pair, and use it as an eviction indicator: the larger the loss, the more important the KV pair. This loss implicitly captures the impact of attention redistribution caused by the removal. Moreover, our empirical observations show that KV importance varies significantly across both time and space. To further improve robustness, we introduce two smoothing mechanisms: (1) an exponential moving average to model temporal dynamics by emphasizing more recent KV pairs, and (2) an adaptive window-based spatial smoothing method, which adjusts for varying window sizes and offsets by estimating the spatial dynamics.

By evaluating on a wide range of downstream tasks including LongBench, RULER, Needle-in-a-Haystack, and InfiniteBench, we demonstrate that ReST-KV consistently outperforms state-of-the-art baselines, especially under low cache budgets and demonstrates more robustness in multi-turn dialogue scenarios. In addition, it reduces decoding latency by up to  $10\times$  at a 128k context length with FlashAttention-2. Notably, it remains fully compatible with existing layer-wise and head-wise budget strategies, enabling seamless integration into current KV cache eviction systems. In summary, we make the following contributions:

- A novel formulation of KV eviction treating as layer-wise output reconstruction, enabling a new importance indicator that captures attention redistribution effects.
- A spatial-temporal smoothing mechanism combining exponential moving average and adaptive windowing, significantly enhancing robustness in KV selection.
- Extensive experiments show that ReST-KV outperforms state-of-the-art baselines under low cache budgets and reduces decoding latency by up to  $10\times$  at a 128k context length.

## 2 Related Work

### 2.1 KV Cache Eviction

KV cache eviction, a prominent method for optimizing KV cache during inference without re-training, alleviates memory and latency issues

in long-context LLMs. Early eviction methods focused on specific attention patterns, such as StreamingLLM (Xiao et al., 2023) and LM-Infinite (Han et al., 2024), retain only the initial and local tokens. While more flexible approaches like FastGen (Ge et al., 2023) and RazorAttention (Tang et al., 2024) were developed, they still rely on predefined patterns and risk ignoring important tokens. Subsequent studies introduced eviction indicators to assess the importance of KV cache entries, often using attention weights. For instance, H2O (Zhang et al., 2023) uses cumulative attention weights, TOVA (Oren et al., 2024) uses the attention weight of the last token, and SnapKV (Li et al., 2024b) pools the average attention weight over the last window. In addition to indicator improvements, some research has explored non-uniform layer-wise and head-wise budget allocation strategies. PyramidKV (Cai et al., 2024) and PyramidInfer (Yang et al., 2024) allocate budget in a pyramid fashion, while DynamicKV (Zhou et al., 2024) and D2O (Wan et al., 2024) adaptively allocate budget based on layer-specific information. AdaKV (Feng et al., 2024) adjusts the budget per head based on output  $\ell_1$  loss bounds. Our work focuses on the limitations of existing eviction indicators, which primarily rely on attention weights derived from query-key interactions and overlook the combined impact of value vectors and spatial-temporal dynamics. Furthermore, our approach is fully compatible with existing layer-wise and head-wise budget allocation strategies.

### 2.2 Attention Dynamics

While attention is central to the success of Transformers, it also poses scalability challenges in long-context settings due to its quadratic complexity. Recent work has therefore investigated attention dynamics—specifically, the spatiotemporal patterns and redistribution of attention weights—as a means to enable more efficient inference.

Several studies reveal structured attention behaviors. MInference (Jiang et al., 2024) discovers a "vertical-slash" pattern, where attention gradually shifts across tokens over time, indicating evolving token importance. FlexPrefill (Lai et al., 2025) similarly identifies consistent attention trajectories during prefill. Keyformer (Adnan et al., 2024) examines how KV eviction distorts attention distributions and proposes normalization to mitigate such shifts.

Distinct from the above methods, we reformulate

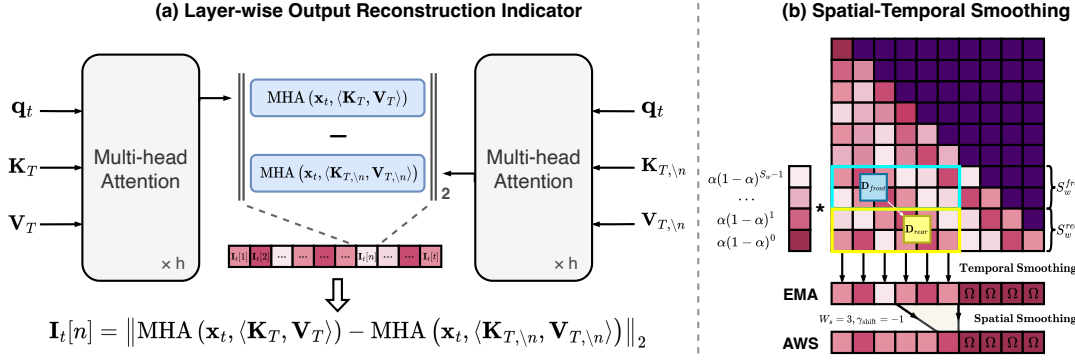


Figure 2: Overview of ReST-KV. (a) Layer-wise output reconstruction quantifies each KV pair’s impact on output error as its eviction indicator. (b) Two smoothing mechanisms enhance robustness: exponential moving average for temporal smoothing and an adaptive window-based approach for spatial smoothing.

KV cache eviction by explicitly modeling attention redistribution and spatiotemporal dynamics. Rather than relying solely on static attention weights, our approach captures temporal evolution and layer-wise shifts in attention, enabling more robust importance estimation and significantly improving performance under memory constraints.

### 3 Methodology

#### 3.1 Preliminary

LLMs typically decode text in an auto-regressive manner, which allows them to generate high-quality, contextually coherent text. However, this decoding process is computationally expensive, as it involves a high degree of repetitive calculations, making it challenging to apply in real-time or large-scale scenarios.

KV cache, a widely recognized and benchmarked technique, reduces redundant computation by storing previously computed keys and values. In this section, we describe the attention computation under the KV cache framework, laying the foundation for our discussion on KV cache eviction. For clarity, we focus on a single attention head and layer, omitting footnotes. At each decoding step  $t$ , the KV cache stores previously computed keys and values  $\langle \mathbf{K}_{1:t-1}, \mathbf{V}_{1:t-1} \rangle$  for  $X[1:t-1]$ , enabling reuse in future steps. For convenience, we denote  $\mathbf{K}_{1:t-1}$  as  $\mathbf{K}_{T-1}$  and  $\mathbf{V}_{1:t-1}$  as  $\mathbf{V}_{T-1}$ . Consequently, the model requires only the current token  $\mathbf{x}_t$  to generate  $\mathbf{x}_{t+1}$ , rather than the full sequence  $X = [\mathbf{x}_1, \dots, \mathbf{x}_t]$ . Formally, at step  $t$ , the query  $\mathbf{q}_t$ , key  $\mathbf{k}_t$ , and value  $\mathbf{v}_t$  are computed as:

$$\mathbf{q}_t = \mathbf{x}_t \mathbf{W}_Q, \mathbf{k}_t = \mathbf{x}_t \mathbf{W}_K, \mathbf{v}_t = \mathbf{x}_t \mathbf{W}_V, \quad (1)$$

where  $\mathbf{W}_Q, \mathbf{W}_K, \mathbf{W}_V$  are the components of the  $\mathbf{Q}, \mathbf{K}, \mathbf{V}$  weight matrices corresponding to a single

attention head. The currently computed  $\mathbf{k}_t$  and  $\mathbf{v}_t$  will be concatenated with the previously cached keys and values, and used in the attention computation for decoding step  $t$ :

$$\mathbf{K}_T = \text{Concat}(\mathbf{K}_{T-1}, \mathbf{k}_t), \mathbf{V}_T = \text{Concat}(\mathbf{V}_{T-1}, \mathbf{v}_t), \quad (2)$$

where  $\mathbf{K}_T$  and  $\mathbf{V}_T$  are the entire sequences of keys and values at decoding step  $t$ . The attention output  $\mathbf{z}_t$  for the token  $\mathbf{x}_t$  at step  $t$  is calculated as:

$$\mathbf{z}_t = \text{softmax} \left( \frac{\mathbf{q}_t \mathbf{K}_T^\top}{\sqrt{d_k}} \right) \mathbf{V}_T = \mathbf{A}_t \mathbf{V}_T, \quad (3)$$

where  $\mathbf{A}_t$  represents the attention weights for the token  $\mathbf{x}_t$  and is used by existing methods to compute eviction indicators.  $d_k$  represents the dimension of the key vectors in the attention mechanism.

Finally, the output of a single head in the multi-head attention can be expressed as:

$$\text{MHA}(\mathbf{x}_t, \langle \mathbf{K}_T, \mathbf{V}_T \rangle) = \mathbf{z}_t \mathbf{W}_O, \quad (4)$$

where  $\mathbf{W}_O$  is the weight matrix of output projection corresponding to a single attention head.

#### 3.2 Layer-wise Reconstruction Indicator

We reformulate KV cache eviction as preserving the attention output distribution at each layer under fixed memory constraints, naturally capturing the effects of attention redistribution. We formalize this paradigm as *layer-wise reconstruction*, a modular framework that aligns with the transformer’s inherent layer-wise computation flow. Specifically, for a single layer, the subproblem is expressed as:

**Definition 3.1.** Given a cache budget  $B$  for a single layer, the task is to select a series of important KV cache entries  $\langle \hat{\mathbf{K}}_T, \hat{\mathbf{V}}_T \rangle$  containing up to  $B$  elements from the total cache entries  $\langle \mathbf{K}_T, \mathbf{V}_T \rangle$  at

the step  $t$ , with the goal of maximizing the retention of the original MHA output. We use  $\ell_2$  distance to calculate reconstruction error, the objective for a single attention head can be defined as:

$$\begin{aligned} \underset{\langle \hat{\mathbf{K}}_T, \hat{\mathbf{V}}_T \rangle}{\operatorname{argmin}} \quad & \left\| \text{MHA}(\mathbf{x}_t, \langle \mathbf{K}_T, \mathbf{V}_T \rangle) - \text{MHA}(\mathbf{x}_t, \langle \hat{\mathbf{K}}_T, \hat{\mathbf{V}}_T \rangle) \right\|_2 \\ \text{s.t.} \quad & |\langle \hat{\mathbf{K}}_T, \hat{\mathbf{V}}_T \rangle| \leq B, \end{aligned} \quad (5)$$

where  $|\langle \hat{\mathbf{K}}_T, \hat{\mathbf{V}}_T \rangle|$  is the number of selected KV pairs.

To efficiently compute Eq.(5), we adopt a greedy selection strategy that retains the top- $B$  KV pairs estimated to have the greatest impact on the attention output. Specifically, for the  $n$ -th KV pair, its importance is measured by the increase in reconstruction error when it is removed, which based on the local linearity assumptions (Molchanov et al., 2016). The eviction indicator is defined as:

$$\mathbf{I}_t[n] = \left\| \text{MHA}(\mathbf{x}_t, \langle \mathbf{K}_T, \mathbf{V}_T \rangle) - \text{MHA}(\mathbf{x}_t, \langle \mathbf{K}_{T \setminus n}, \mathbf{V}_{T \setminus n} \rangle) \right\|_2, \quad (6)$$

where  $\langle \mathbf{K}_{T \setminus n}, \mathbf{V}_{T \setminus n} \rangle$  represents the set of cache with the  $n$ -th KV pair removed.

By introducing Eq. (3) and Eq. (4) for derivation, Eq. (6) can be simplified as follows:

$$\mathbf{I}_t[n] = \frac{\mathbf{A}_t[n]}{1 - \mathbf{A}_t[n]} \left\| \text{MHA}(\mathbf{x}_t, \langle \mathbf{K}_T, \mathbf{V}_T \rangle) - \mathbf{v}_n \mathbf{W}_O \right\|_2, \quad (7)$$

where  $\mathbf{A}_t[n]$  represents the attention weights of the query  $\mathbf{q}_t$  with respect to the key  $\mathbf{k}_n$ , and  $\mathbf{v}_n$  represents the  $n$ -th value in the value cache  $\mathbf{V}_T$ .

Traditional eviction indicators only considered  $\mathbf{A}_t[n]$ , neglecting the effects of attention redistribution. Eq. (7) demonstrates that the importance of a KV pair depends on two mechanisms:

- **Nonlinear Attention Reweighting:** The first term  $\frac{\mathbf{A}_t[n]}{1 - \mathbf{A}_t[n]}$  acts as a monotonic nonlinear amplifier in  $(0, 1)$ . While preserving the conventional principle that higher attention weights  $\mathbf{A}_t[n]$  indicate stronger retention priority, this transformation introduces curvature to better discriminate between high-competition KV pairs compared to linear scaling in prior methods.
- **Redistribution Sensitivity:** The second term  $\left\| \text{MHA}(\cdot) - \mathbf{v}_n \mathbf{W}_O \right\|_2$  captures the redistribution of attention after removing the  $n$ -th KV pair. It reflects how much the remaining KV pairs fail to compensate for the excluded value in reconstructing the MHA output. A smaller discrepancy indicates that attention can be effectively redistributed to preserve the output, thus signaling lower importance of the removed KV pair.

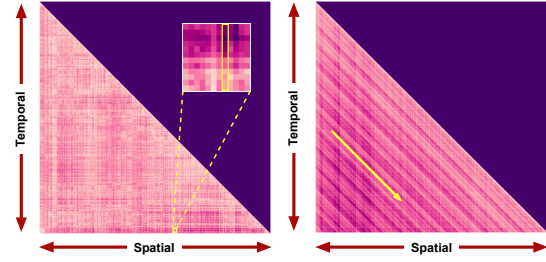


Figure 3: Visualization analysis of the spatial-temporal dynamics of the output reconstruction indicator. The left plot shows dynamic temporal variations in KV pair importance over steps, with the zoomed-in view highlighting a KV pair’s gradual decline in importance. The right plot reveals spatial shifts, where similar importance patterns emerge at shifted positions.

The additional analysis and the derivation of Eq. (7) can be found in Appendix A and Eq. (21).

### 3.3 Spatial-Temporal Smoothing

To enhance the robustness of KV pair selection during the prefill stage, we analyze the spatial-temporal dynamics of the KV pairs’ reconstruction error (Eq. (7)). From Figure 3, we observe two key characteristics: (1) The importance of KV pairs exhibits dynamic temporal variations (i.e., the fluctuating patterns of  $\mathbf{I}_1[n], \mathbf{I}_2[n], \dots, \mathbf{I}_t[n]$  along the temporal dimension, and (2) simultaneously demonstrates dynamic spatial shifts where similar importance distributions emerge across shifted positions (e.g.,  $\mathbf{I}_{t-k}[n-kN], \dots, \mathbf{I}_{t-1}[n-N], \mathbf{I}_t[n]$  exhibit analogous patterns).

Leveraging these observations, we introduce two novel smoothing mechanisms to enhance the robustness of KV pair selection, as illustrated in Figure 2(b). These mechanisms address temporal variations and spatial shifts in KV pair importance, ensuring a more stable and reliable selection process. By applying these techniques, we aim to reduce short-term fluctuations and capture long-term trends, ultimately improving the performance of the KV cache eviction.

#### Exponential Moving Average Temporal Smoothing.

Inspired by SnapKV (Li et al., 2024b), we use a recent query window  $S_w$  to assess the importance of KV pairs. To model temporal dynamics, we apply exponential moving average (EMA) smoothing to the importance of KV pairs, which assigns higher weights to recent queries while dampening earlier fluctuations. To apply this smoothing over a limited window of recent queries, we define the temporal smoothing as:

$$\hat{\mathbf{I}}_t[n] = \begin{cases} \text{EMA}(\mathbf{I}_{t-S_w:t}[n]), & \text{if } n < t - S_w, \\ \Omega, & \text{otherwise,} \end{cases} \quad (8)$$



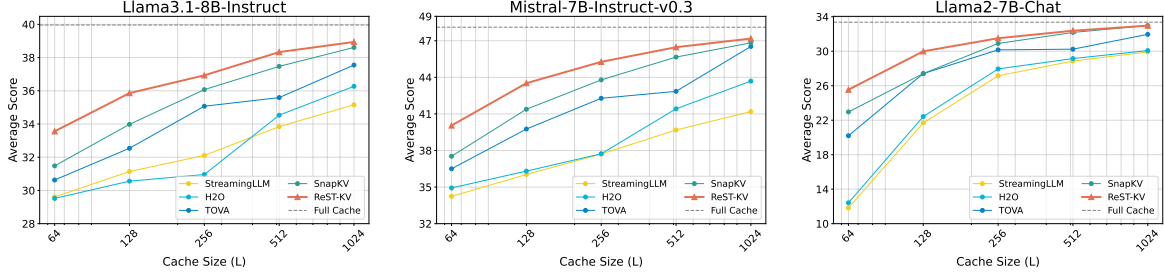


Figure 4: Average score across 16 datasets of LongBench under various cache budgets. ReST-KV outperforms the baseline across different models and settings.

where  $\hat{\mathbf{I}}_t[n]$  represents the eviction indicator with temporal smoothing.  $\text{EMA}(\cdot)$  captures the temporal variation in importance. We assign an arbitrarily large value  $\Omega$  to the most recent  $S_w$  tokens to ensure their preservation.

The exponential moving average  $\text{EMA}(\cdot)$  is defined as:

$$\text{EMA}(\mathbf{I}_{t_1:t_2}[n]) = \begin{cases} \alpha \mathbf{I}_{t_2}[n] + (1 - \alpha) \text{EMA}(\mathbf{I}_{t_1:t_2-1}[n]), & \text{if } t_1 < t_2, \\ \mathbf{I}_{t_1}[n], & \text{elif } t_1 = t_2, \end{cases} \quad (9)$$

where  $\text{EMA}(\mathbf{I}_{t_1:t_2}[n])$  represents the exponential moving average of the reconstruction errors  $\mathbf{I}_{t_1}[n], \dots, \mathbf{I}_{t_2}[n]$  computed over the steps from  $t_1$  to  $t_2$ .  $\alpha$  is the smoothing factor that controls the weight of the current reconstruction error  $\mathbf{I}_{t_2}[n]$  relative to the previous error  $\text{EMA}(\mathbf{I}_{t_1:t_2-1}[n])$  in the update process.

#### Adaptive Window-Based Spatial Smoothing.

To capture spatial shifts in KV importance over time, we split the observation window into two halves:  $S_w^{\text{front}}$  and  $S_w^{\text{rear}}$ . For each half, we compute the average index of the top- $B$  important KV pairs:

$$\mathbf{D}_{\text{front}} = \frac{2}{B \cdot S_w} \sum_{t \in S_w^{\text{front}}} \sum_B \arg\max_B(\mathbf{I}_t), \quad (10)$$

where  $\frac{2}{B \cdot S_w}$  is a normalization factor.  $S_w^{\text{front}}$  denotes the first half of queries within the input window  $S_w$ .  $\mathbf{D}_{\text{rear}}$  is computed similarly for the second half of the queries. The difference  $\Delta D = \mathbf{D}_{\text{rear}} - \mathbf{D}_{\text{front}}$  reflects how KV importance shifts across positions. We use this signal to adaptively adjust both the window size and shift:

$$W_s = 2 \cdot \left\lfloor \frac{|\mathbf{D}_{\text{rear}} - \mathbf{D}_{\text{front}}|}{\beta} \right\rfloor + 1, \quad (11)$$

$$\gamma_{\text{shift}} = \begin{cases} \left\lfloor \frac{\mathbf{D}_{\text{front}} - \mathbf{D}_{\text{rear}}}{\beta} \right\rfloor, & \text{if } \mathbf{D}_{\text{front}} - \mathbf{D}_{\text{rear}} > 0, \\ \left\lfloor \frac{\mathbf{D}_{\text{rear}} - \mathbf{D}_{\text{front}}}{\beta} \right\rfloor + 1, & \text{if } \mathbf{D}_{\text{front}} - \mathbf{D}_{\text{rear}} \leq 0, \end{cases} \quad (12)$$

where  $W_s$  is the window size and  $\gamma_{\text{shift}}$  is the shift of the sliding window.  $\beta$  is a scaling factor that

determines the granularity of the sliding window's movement, controlling the size of the steps taken when calculating the window shift and size.  $\lfloor \cdot \rfloor$  represents the floor function, which rounds a number down to the nearest integer.

In summary, the final eviction indicator, which incorporates both layer-wise output reconstruction and spatial-temporal smoothing, is as follows:

$$\mathcal{I}_t[n] = \frac{\sum_{k=-\lfloor W_s/2 \rfloor + \gamma_{\text{shift}}}^{\lfloor W_s/2 \rfloor + \gamma_{\text{shift}}} \hat{\mathbf{I}}_t[k]}{W_s}. \quad (13)$$

The selected  $\langle \hat{\mathbf{K}}_T, \hat{\mathbf{V}}_T \rangle$  is the subset of the original KV pairs, defined as:

$$\hat{\mathbf{K}}_T = \mathbf{K}_T[\mathbf{D}_t, :], \hat{\mathbf{V}}_T = \mathbf{V}_T[\mathbf{D}_t, :], \mathbf{D}_t = \arg\max_B(\mathcal{I}_t), \quad (14)$$

where  $\mathbf{D}_t$  denotes the indices of the top  $B$  KV pairs based on the eviction indicator  $\mathcal{I}_t$ . The same operation is applied to each head and layer, and different KV pairs can be selected for different heads in each layer.

## 4 Experiments

### 4.1 Experimental Settings

**Backbone LLMs.** We evaluate ReST-KV on five open-source LLMs spanning two mainstream attention architectures: (1) **Multi-head attention**, Llama2-Chat (Touvron et al., 2023) and Gemma-Instruct (Team et al., 2024); (2) **Grouped-query attention**, Llama3-Instruct (Dubey et al., 2024), Mistral-Instruct-v0.3 (Jiang et al., 2023), and Qwen2.5-Instruct (Team, 2024).

**Baseline Methods.** We compare ReST-KV with four baselines: (1) Fixed Attention Patterns: StreamingLLM (Xiao et al., 2023); (2) Eviction Indicator: H2O (Zhang et al., 2023), TOVA (Oren et al., 2024), SnapKV (Li et al., 2024b). We also incorporate adaptive budget strategies from PyramidKV (Cai et al., 2024) and AdaKV (Feng et al., 2024) into our method to show compatibility.

Table 1: Performance comparison across 16 datasets of LongBench. The best result is highlighted in **bold**, and the second-best is underlined. ReST-KV achieves the best performance in most cases.

Method	Single-Document QA			Multi-Document QA			Summarization			Few-shot Learning			Synthetic		Code		Avg.
	NrtvQA	Qasper	MF-en	HotpotQA	2WikiMQA	Musique	GovReport	QMSum	MultiNews	TREC	TriviaQA	SAMSum	PCount	PRE	Lcc	RB-P	
Llama-3.1-8B-Instruct, $B_{\text{total}} = 64L$																	
StreamingLLM	7.65	5.08	14.14	10.93	12.64	6.86	16.57	18.93	16.30	38.50	83.13	34.65	<b>9.78</b>	<b>96.28</b>	54.16	48.21	29.61
H2O	12.23	5.12	15.12	11.51	10.14	6.23	17.23	19.51	16.79	39.15	81.51	36.12	8.12	95.12	51.25	47.12	29.52
TOVA	18.52	<u>6.12</u>	17.32	12.15	12.51	7.35	16.24	20.41	16.34	38.41	82.61	36.16	8.14	<u>95.23</u>	<u>55.21</u>	47.35	30.63
SnapKV	<u>19.90</u>	5.78	<u>18.38</u>	<u>13.51</u>	<u>14.42</u>	<b>8.52</b>	<u>17.35</u>	<u>20.44</u>	<u>17.33</u>	<u>41.00</u>	<u>85.37</u>	<u>37.63</u>	<u>8.93</u>	91.08	55.09	<b>48.88</b>	<u>31.48</u>
ReST-KV	<b>22.43</b>	<b>7.19</b>	<b>19.25</b>	<b>14.11</b>	<b>15.04</b>	<u>7.97</u>	<b>20.56</b>	<b>21.10</b>	<b>19.15</b>	<b>53.50</b>	<b>88.23</b>	<b>40.21</b>	8.46	93.90	<b>56.74</b>	<u>48.77</u>	<b>33.54</b>
Llama-3.1-8B-Instruct, $B_{\text{total}} = 512L$																	
StreamingLLM	19.15	6.47	15.02	10.94	12.58	6.23	23.66	20.05	23.31	57.50	87.70	<u>41.86</u>	<b>10.25</b>	90.74	62.39	53.61	33.84
H2O	26.23	7.34	20.51	11.52	13.52	7.34	23.23	21.24	23.14	58.50	86.12	40.15	7.25	91.02	61.23	54.12	34.53
TOVA	27.34	8.34	22.45	12.25	14.51	8.42	24.23	22.13	22.25	58.50	89.31	40.51	8.24	93.14	62.23	55.61	35.59
SnapKV	<u>28.02</u>	<u>9.83</u>	<u>24.84</u>	<u>13.77</u>	<u>15.40</u>	<u>10.21</u>	<u>25.13</u>	<u>22.73</u>	<u>24.25</u>	<u>65.00</u>	<b>92.34</b>	41.69	<u>8.42</u>	<u>96.31</u>	<b>64.30</b>	<b>57.28</b>	<u>37.47</u>
ReST-KV	<b>32.01</b>	<b>10.73</b>	<b>25.23</b>	<b>15.91</b>	<b>15.85</b>	<b>10.25</b>	<b>26.47</b>	<b>23.23</b>	<b>24.79</b>	<b>69.00</b>	91.62	<b>42.59</b>	8.40	<b>97.66</b>	63.48	56.03	<b>38.33</b>
Full	32.02	13.12	27.52	16.60	16.41	11.41	34.59	23.41	26.89	73.00	91.65	43.80	7.18	97.73	65.12	58.89	39.96
Mistral-7B-Instruct-v0.3, $B_{\text{total}} = 64L$																	
StreamingLLM	20.37	20.56	24.62	38.87	32.47	17.68	15.48	19.84	15.81	<u>39.50</u>	82.77	36.72	5.50	80.00	49.77	47.90	34.24
H2O	20.51	21.52	25.12	40.12	33.12	18.34	16.23	19.12	16.24	38.50	83.12	37.23	6.00	85.50	50.12	48.12	34.93
TOVA	<u>22.51</u>	22.24	37.23	41.12	34.10	19.52	17.21	19.23	16.27	38.50	85.12	38.51	<u>6.50</u>	<u>86.50</u>	51.04	48.42	36.50
SnapKV	19.39	<u>23.62</u>	<u>38.66</u>	<u>43.26</u>	<u>34.72</u>	<u>21.33</u>	<u>17.59</u>	<u>20.93</u>	<u>17.06</u>	38.50	86.96	<u>39.61</u>	<b>7.00</b>	<b>90.50</b>	<u>51.63</u>	<u>49.73</u>	<u>37.53</u>
ReST-KV	<b>25.65</b>	<b>26.58</b>	<b>42.71</b>	<b>46.11</b>	<b>36.43</b>	<b>24.34</b>	<b>19.80</b>	<b>21.65</b>	<b>18.90</b>	<b>51.50</b>	<b>87.88</b>	<b>41.54</b>	4.00	<b>90.50</b>	<b>52.39</b>	<b>50.75</b>	<b>40.05</b>
Mistral-7B-Instruct-v0.3, $B_{\text{total}} = 512L$																	
StreamingLLM	24.19	25.97	30.14	40.75	31.90	17.35	22.18	20.30	23.22	65.50	86.95	43.75	<b>6.00</b>	81.00	59.35	56.36	39.68
H2O	25.23	30.41	40.32	42.52	35.23	18.23	24.23	21.24	23.21	66.50	86.71	43.15	5.00	82.52	<u>60.13</u>	58.15	41.42
TOVA	25.23	32.52	46.24	45.23	36.23	20.32	24.53	22.53	23.64	66.50	87.24	44.21	<b>6.00</b>	<u>85.62</u>	59.35	60.24	42.85
SnapKV	<u>26.84</u>	<u>35.51</u>	<u>53.12</u>	<b>49.56</b>	<u>37.72</u>	<u>26.54</u>	<u>25.06</u>	<u>24.03</u>	<u>24.76</u>	<u>67.50</u>	<u>89.36</u>	<u>44.82</u>	<u>5.50</u>	<b>98.50</b>	<b>60.44</b>	<b>61.22</b>	<u>45.66</u>
ReST-KV	<b>28.60</b>	<b>35.86</b>	<b>53.37</b>	<u>49.13</u>	<b>38.70</b>	<b>27.94</b>	<b>26.05</b>	<b>24.37</b>	<b>25.09</b>	<b>73.50</b>	<b>89.66</b>	<b>46.27</b>	<u>5.50</u>	<b>98.50</b>	<u>60.13</u>	<u>60.84</u>	<b>46.47</b>
Full	29.07	41.54	52.88	49.37	39.01	28.58	35.07	25.71	27.73	76.00	88.59	47.51	6.00	98.50	61.48	62.68	48.11

**Evaluating Tasks.** We evaluate ReST-KV on three prominent benchmarks: (1) LongBench (Bai et al., 2023), which tests long-context understanding across 16 datasets spanning six categories; and (2) RULER (Hsieh et al., 2024), a challenging long-context benchmark consisting of 4 categories and 13 complex tasks; (3) Needle-in-a-Haystack (Liu et al., 2024a), designed to assess the ability of models to retrieve key information from long sequences; (4) InfiniteBench (Zhang et al., 2024b), includes 10 tasks designed to test various aspects of long-context processing. Detailed results are reported in Appendix J.

**Implementation Details.** We evaluate ReST-KV and all baselines under varying cache budgets ( $B_{\text{total}} = nL$ , with  $n \in [64, 1024]$ ), where  $n$  denotes the number of KV pairs per layer across  $L$  layers. To ensure fairness, token eviction is performed only once during the prefilling phase. All methods, except TOVA, are implemented based on the codebase from (Cai, 2023). Experiments are run on NVIDIA A800 80GB GPUs. Further details are provided in Appendix B.

## 4.2 Evaluations on LongBench Dataset

We evaluate ReST-KV on 16 datasets from LongBench. As shown in Figure 4, ReST-KV consistently outperforms all baselines across different

cache budget settings, with especially strong gains under tight memory constraints. Unlike prior methods that rely solely on the rank of query-key similarities, our approach accounts the impact of attention redistribution, ensuring that the most critical information is retained. Moreover, we verify the compatibility of ReST-KV with non-uniform budget strategies such as PyramidKV and AdaKV, with results presented in Appendix C. Compatibility with KV cache quantization techniques is also evaluated, as shown in Appendix I.

Table 1 provides a detailed comparison under two cache budgets: low ( $B_{\text{total}} = 64L$ ) and high ( $B_{\text{total}} = 512L$ ), with full results in Appendix D.1. ReST-KV consistently ranks among the top performers across tasks, achieving up to a 2.58% improvement under low budgets with the Mistral model. These results highlight the effectiveness of our eviction indicator and spatio-temporal smoothing in enhancing KV selection robustness. Additional evaluations across different models and sizes further confirm this conclusion (Appendix D.2, D.3).

## 4.3 Evaluations on RULER Benchmark

We evaluate ReST-KV on 11 tasks from the RULER benchmark using the Llama3.1-8B-Instruct model, with a fixed cache budget of

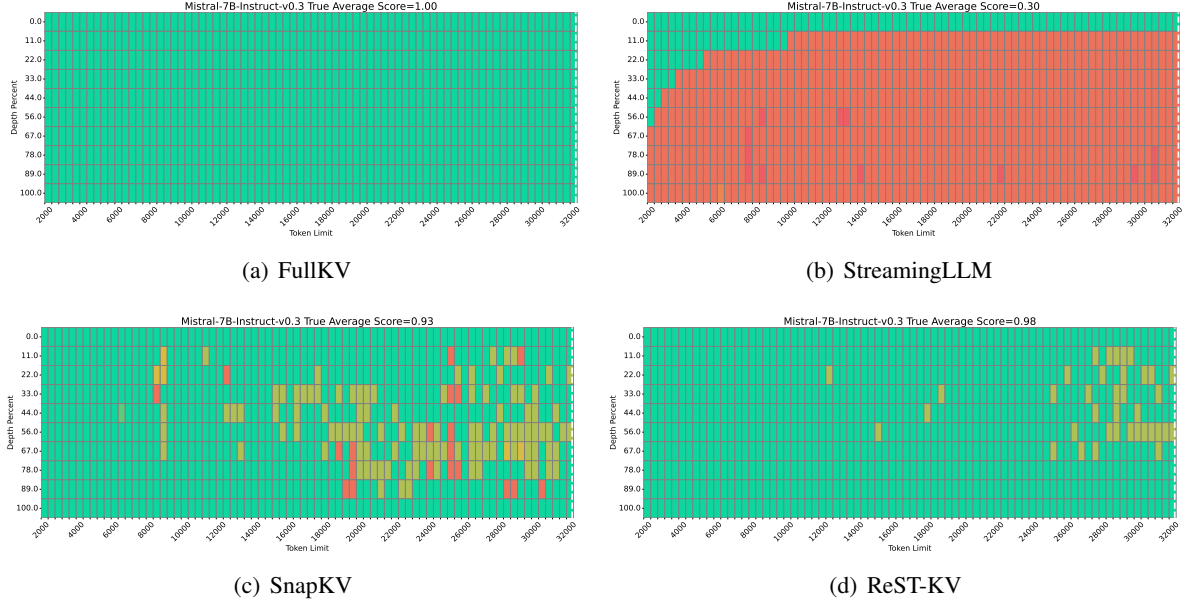


Figure 5: Performance comparison on the Needle in a Haystack Test using Mistral-7B-Instruct-v0.3 with  $B_{\text{total}} = 1024L$ . Even with a strict cache budget, ReST-KV retains 98% of the model’s performance, outperforming other methods in retrieving critical information.

$B_{\text{total}} = 1024L$  applied across all methods. Table 2 summarizes the average accuracy across varying context lengths, from 4k to 128k context length. Existing KV cache eviction methods suffer from substantial performance degradation as the context length increases, highlighting their limited robustness in long-context and complex retrieval scenarios. In contrast, ReST-KV consistently achieves strong results across all lengths, with an average accuracy improvement of 15.3% over prior methods. Notably, even at the 128k context length—where less than 1% of the original cache is retained—ReST-KV maintains effective retrieval capabilities. Detailed results for individual tasks are provided in Appendix E.

Table 2: Performance comparison on RULER benchmark across different context lengths. ReST-KV demonstrates robust performance across all lengths.

Method	4K	8K	16K	32K	64K	128K	Avg.
Streaming	39.81	18.42	12.10	10.57	9.91	8.18	16.50
SnapKV	83.60	75.54	71.12	66.95	57.47	47.99	67.11
PyramidKV	81.35	73.66	70.23	69.83	57.84	48.93	66.97
ReST-KV	<b>94.01</b>	<b>86.66</b>	<b>84.12</b>	<b>81.87</b>	<b>78.65</b>	<b>68.28</b>	<b>82.27</b>
Full	99.34	98.83	98.55	94.89	89.85	79.32	93.46

#### 4.4 Visualization on NIAH Test

The needle-in-a-haystack test (Liu et al., 2024a) involves inserting key information at random positions within long contexts and serves as a benchmark to assess the ability of LLMs to accurately retrieve critical information. To further demonstrate the effectiveness and adaptability of our

method, we conducted experiments on the Mistral-7B-Instruct-v0.3 model with a cache budget set to  $B_{\text{total}} = 1024L$ . As shown in Figure 5, even under such a strict cache budget, ReST-KV maintains 98% of the model’s performance, significantly outperforming other methods. This underscores ReST-KV’s ability to efficiently prioritize and retain the most relevant KV pairs. Additional visualization graphs can be found in Appendix F.

#### 4.5 Ablation Studies

We conduct ablation studies on LongBench to evaluate the contribution of each component in our KV cache management strategy: layer-wise output reconstruction (LOR) indicator, exponential moving average (EMA) temporal smoothing, and adaptive window-based spatial smoothing (AWS). We adopt the Llama3.1-8B-Instruct model with a cache budget of  $B_{\text{total}} = 128L$  as the default configuration.

Table 3: Ablation results of ReST-KV. LOR means layer-wise output reconstruction indicator. EMA means exponential moving average temporal smoothing. AWS means adaptive window-based spatial smoothing.

Method	Avg. Acc
Vanilla Attention weight Top-k	32.98
<b>ReST-KV</b>	<b>35.86</b>
ReST-KV w/o LOR	33.95 (-1.91)
ReST-KV w/o EMA	34.02 (-1.84)
ReST-KV w/o AWS	33.50 (-2.36)

Table 3 systematically presents the results. The baseline using vanilla attention-weight-based top-

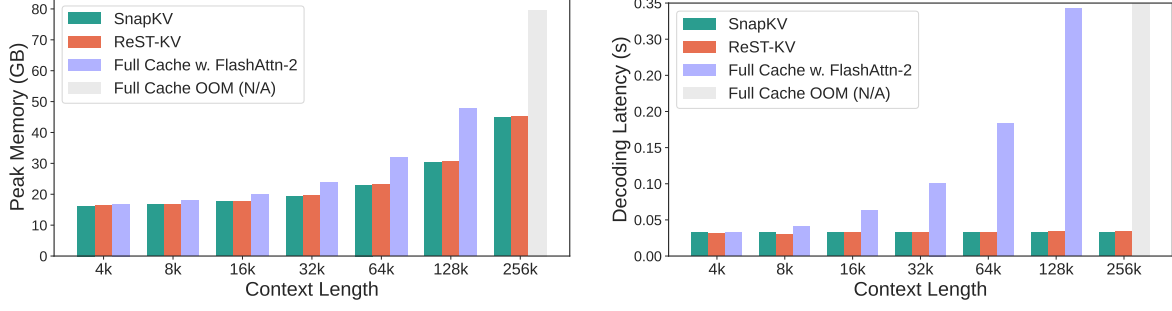


Figure 6: Peak memory usage and decoding latency on NVIDIA A800 80GB GPU. ReST-KV reduces peak memory by 36.0% and achieves up to a 10 $\times$  speedup at 128k context length compared to full cache.

$k$  selection yields only 32.98 accuracy, as it ignores attention redistribution and fails to capture the spatial-temporal dynamics of KV pairs. In contrast, our ReST-KV framework achieves 35.86 accuracy, representing a significant improvement.

To further understand the effectiveness of each module, we ablate them individually:

- Without the LOR indicator, the model misses attention redistribution effects, making it harder to identify truly critical KV pairs. This is especially harmful under tight budgets like  $B_{\text{total}} = 128L$ , causing a 1.91% drop in accuracy.
- Without EMA temporal smoothing: The model lacks awareness of temporal changes in importance, making it less capable of retaining KV pairs crucial for future queries. This results in a 1.84% performance degradation.
- Without AWS spatial smoothing: Without capturing spatial offset patterns (e.g., vertical-slash structures), the model tends to retain suboptimal KV pairs, causing a 2.36% accuracy drop.

Detailed ablation of each module and sensitivity analysis can be found in Appendix G.

#### 4.6 Evaluation of Memory and Throughput

To evaluate the effectiveness and efficiency of our method in reducing memory consumption and enhancing LLM inference, we analyze peak memory usage and decoding latency on the Llama-3.1-8B-Instruct model implemented with FlashAttention-2 (Dao, 2023).

**Peak Memory Usage.** As shown in Figure 6(a), ReST-KV significantly reduces peak memory usage, performing comparably to other KV cache eviction methods. Compared to full cache, ReST-KV achieves approximately 36.0% reduction in peak memory usage at a context length of 128k.

**Throughput Analysis.** As shown in Figure 6(b), as the input length increases, the decoding latency

rises significantly due to the growing computational demands and I/O latency bottlenecks. Even with FlashAttention-2 acceleration, the decoding latency of the full cache method continues to increase rapidly with longer input lengths. In contrast, ReST-KV effectively reduces the number of KV pairs required by maintaining a fixed cache budget, alleviating the decoding latency for long inputs. Notably, when processing sequences with a context length of 128K, ReST-KV achieves a speedup of approximately 10 $\times$  compared to the full cache method, significantly improving inference efficiency.

Moreover, ReST-KV is compatible with prefill sparse attention approaches, enabling substantial reduction in time-to-first-token (TTFT); see Appendix H for details.

## 5 Conclusion

In this paper, we propose ReST-KV, a novel KV cache eviction method that reformulates eviction as a layer-wise output reconstruction task, effectively capturing attention redistribution effects beyond conventional attention-weight heuristics. To enhance robustness, ReST-KV integrates a spatial-temporal smoothing mechanism using exponential moving averages for temporal stability and adaptive windowing for spatial awareness. Extensive evaluations on LongBench, Needle-in-a-Haystack, and RULER demonstrate that ReST-KV consistently surpasses state-of-the-art methods under low memory budgets and significantly reduces decoding latency—achieving up to 10 $\times$  speedups at 128k context lengths. Our method is model-agnostic and compatible with existing budget strategies, offering a practical and principled solution for efficient long-context generative inference. Future work will explore tighter integration with adaptive allocation strategies and extensions to multi-modal or structured memory scenarios.



## 6 Limitations

While our proposed ReST-KV demonstrates strong performance across standard long-context benchmarks, several limitations warrant discussion.

First, our experiments are primarily conducted on English-language datasets and LLMs. The generalizability of our method to multilingual scenarios or models trained on diverse linguistic corpora remains to be validated. Additionally, although ReST-KV is designed to be model-agnostic, its effectiveness in non-text modalities—such as vision-language or structured memory settings—has not yet been explored.

Second, our evaluation focuses on long-context modeling and retrieval tasks using benchmarks such as LongBench, RULER, and Needle-in-a-Haystack. These tasks assess the model’s ability to retain and access relevant information under constrained memory budgets. However, more cognitively complex tasks—such as multi-step reasoning, long-form tool use, or multi-turn chain-of-thought generation—may exhibit different sensitivity to KV cache eviction strategies. The impact of ReST-KV on such advanced reasoning capabilities is still unclear and should be explored in future work.

Third, while ReST-KV introduces only minor computational overhead compared to prior methods like SnapKV and PyramidKV, this comes at the cost of increased reconstruction steps per eviction decision. Although our method preserves the same asymptotic complexity, further optimization may be needed for deployment in real-time or latency-sensitive systems.

Finally, despite achieving a 15.3% accuracy improvement on average over prior SOTA on the RULER benchmark, the performance gap between our method and full-cache baselines remains notable, especially in multi-turn dialogue settings such as MK-NIAH-3. This highlights potential areas for improvement in modeling long-range dependencies in conversational memory.

## References

- Josh Achiam, Steven Adler, Sandhini Agarwal, Lama Ahmad, Ilge Akkaya, Florencia Leoni Aleman, Diogo Almeida, Janko Altschmidt, Sam Altman, Shyamal Anadkat, and 1 others. 2023. Gpt-4 technical report. *arXiv preprint arXiv:2303.08774*.
- Muhammad Adnan, Akhil Arunkumar, Gaurav Jain, Prashant J Nair, Ilya Soloveychik, and Purushotham Kamath. 2024. Keyformer: Kv cache reduction

through key tokens selection for efficient generative inference. *Proceedings of Machine Learning and Systems*, 6:114–127.

Anthropic. 2023. [Claude 3: A next-generation language model](#). Accessed: 2025-01-21.

Yushi Bai, Xin Lv, Jiajie Zhang, Hongchang Lyu, Jiankai Tang, Zhidian Huang, Zhengxiao Du, Xiao Liu, Aohan Zeng, Lei Hou, and 1 others. 2023. Longbench: A bilingual, multitask benchmark for long context understanding. *arXiv preprint arXiv:2308.14508*.

Zefan Cai. 2023. [Kvcache-factory](#). Accessed: 2025-01-21.

Zefan Cai, Yichi Zhang, Bofei Gao, Yuliang Liu, Tianyu Liu, Keming Lu, Wayne Xiong, Yue Dong, Baobao Chang, Junjie Hu, and 1 others. 2024. Pyramidkv: Dynamic kv cache compression based on pyramidal information funneling. *arXiv preprint arXiv:2406.02069*.

Tri Dao. 2023. Flashattention-2: Faster attention with better parallelism and work partitioning. *arXiv preprint arXiv:2307.08691*.

Zhengxiao Du, Yujie Qian, Xiao Liu, Ming Ding, Jiezhong Qiu, Zhilin Yang, and Jie Tang. 2021. Glm: General language model pretraining with autoregressive blank infilling. *arXiv preprint arXiv:2103.10360*.

Abhimanyu Dubey, Abhinav Jauhri, Abhinav Pandey, Abhishek Kadian, Ahmad Al-Dahle, Aiesha Letman, Akhil Mathur, Alan Schelten, Amy Yang, Angela Fan, and 1 others. 2024. The llama 3 herd of models. *arXiv preprint arXiv:2407.21783*.

Yuan Feng, Junlin Lv, Yukun Cao, Xike Xie, and S Kevin Zhou. 2024. Ada-kv: Optimizing kv cache eviction by adaptive budget allocation for efficient llm inference. *arXiv preprint arXiv:2407.11550*.

Suyu Ge, Yunan Zhang, Liyuan Liu, Minjia Zhang, Jiawei Han, and Jianfeng Gao. 2023. Model tells you what to discard: Adaptive kv cache compression for llms. *arXiv preprint arXiv:2310.01801*.

Zhiyu Guo, Hidetaka Kamigaito, and Taro Watanabe. 2024. Attention score is not all you need for token importance indicator in kv cache reduction: Value also matters. *arXiv preprint arXiv:2406.12335*.

Chi Han, Qifan Wang, Hao Peng, Wenhan Xiong, Yu Chen, Heng Ji, and Sinong Wang. 2024. [Lm-infinite: Zero-shot extreme length generalization for large language models](#). *Preprint*, arXiv:2308.16137.

Coleman Hooper, Sehoon Kim, Hiva Mohammadzadeh, Michael W Mahoney, Sophia Shao, Kurt Keutzer, and Amir Gholami. 2024. Kvquant: Towards 10 million context length llm inference with kv cache quantization. *Advances in Neural Information Processing Systems*, 37:1270–1303.

667	Cheng-Ping Hsieh, Simeng Sun, Samuel Kriman, Shan-	Hanlin Tang, Yang Lin, Jing Lin, Qingsen Han, Shikuan	723
668	tanu Acharya, Dima Rekesh, Fei Jia, Yang Zhang,	Hong, Yiwu Yao, and Gongyi Wang. 2024. Razo-	724
669	and Boris Ginsburg. 2024. Ruler: What’s the real	rattention: Efficient kv cache compression through	725
670	context size of your long-context language models?	retrieval heads. <i>arXiv preprint arXiv:2407.15891</i> .	726
671	<i>arXiv preprint arXiv:2404.06654</i> .		
672	Albert Q Jiang, Alexandre Sablayrolles, Arthur Men-	Gemma Team, Thomas Mesnard, Cassidy Hardin,	727
673	sch, Chris Bamford, Devendra Singh Chaplot, Diego	Robert Dadashi, Surya Bhupatiraju, Shreya Pathak,	728
674	de las Casas, Florian Bressand, Gianna Lengyel, Guil-	Laurent Sifre, Morgane Rivi�re, Mihir Sanjay Kale,	729
675	laume Lample, Lucile Saulnier, and 1 others. 2023.	Juliette Love, and 1 others. 2024. Gemma: Open	730
676	Mistral 7b. <i>arXiv preprint arXiv:2310.06825</i> .	models based on gemini research and technology.	731
		<i>arXiv preprint arXiv:2403.08295</i> .	732
677	Huiqiang Jiang, Yucheng Li, Chengruidong Zhang,	Qwen Team. 2024. Qwen2. 5: A party of foundation	733
678	Qianhui Wu, Xufang Luo, Surin Ahn, Zhenhua Han,	models. <i>Qwen (Sept. 2024)</i> . url: <a href="https://qwenlm.github.io/blog/qwen2,5">https://qwenlm.</a>	734
679	Amir Abdi, Dongsheng Li, Chin-Yew Lin, and 1 oth-	<i>github.io/blog/qwen2,5</i> .	735
680	ers. 2024. Minference 1.0: Accelerating pre-filling		
681	for long-context llms via dynamic sparse attention.	Hugo Touvron, Louis Martin, Kevin Stone, Peter Al-	736
682	<i>Advances in Neural Information Processing Systems</i> ,	bert, Amjad Almahairi, Yasmine Babaei, Nikolay	737
683	37:52481–52515.	Bashlykov, Soumya Batra, Prajjwal Bhargava, Shruti	738
684	Xunhao Lai, Jianqiao Lu, Yao Luo, Yiyuan Ma, and	Bhosale, and 1 others. 2023. Llama 2: Open foun-	739
685	Xun Zhou. 2025. Flexprefill: A context-aware sparse	dation and fine-tuned chat models. <i>arXiv preprint</i>	740
686	attention mechanism for efficient long-sequence in-	<i>arXiv:2307.09288</i> .	741
687	ference. <i>arXiv preprint arXiv:2502.20766</i> .		
688	Haoyang Li, Yiming Li, Anxin Tian, Tianhao Tang,	Zhongwei Wan, Xinjian Wu, Yu Zhang, Yi Xin, Chaofan	742
689	Zhanchao Xu, Xuejia Chen, Nicole Hu, Wei Dong,	Tao, Zhihong Zhu, Xin Wang, Siqi Luo, Jing Xiong,	743
690	Qing Li, and Lei Chen. 2024a. A survey on large	and Mi Zhang. 2024. D2o: Dynamic discriminative	744
691	language model acceleration based on kv cache man-	operations for efficient generative inference of large	745
692	agement. <i>arXiv preprint arXiv:2412.19442</i> .	language models. <i>arXiv preprint arXiv:2406.13035</i> .	746
693	Yuhong Li, Yingbing Huang, Bowen Yang, Bharat	Guangxuan Xiao, Yuandong Tian, Beidi Chen, Song	747
694	Venkitesh, Acyr Locatelli, Hanchen Ye, Tianle Cai,	Han, and Mike Lewis. 2023. Efficient streaming	748
695	Patrick Lewis, and Deming Chen. 2024b. Snapkv:	language models with attention sinks. <i>arXiv preprint</i>	749
696	Llm knows what you are looking for before genera-	<i>arXiv:2309.17453</i> .	750
697	tion. <i>arXiv preprint arXiv:2404.14469</i> .		
698	Nelson F Liu, Kevin Lin, John Hewitt, Ashwin Paranjape,	Dongjie Yang, XiaoDong Han, Yan Gao, Yao Hu, Shilin	751
699	Michele Bevilacqua, Fabio Petroni, and Percy	Zhang, and Hai Zhao. 2024. Pyramidinfer: Pyra-	752
700	Liang. 2024a. Lost in the middle: How language	mid kv cache compression for high-throughput llm	753
701	models use long contexts. <i>Transactions of the Asso-</i>	inference. <i>arXiv preprint arXiv:2405.12532</i> .	754
702	<i>ciation for Computational Linguistics</i> , 12:157–173.		
703	Zirui Liu, Jiayi Yuan, Hongye Jin, Shaochen Zhong,	Shunyu Yao, Jeffrey Zhao, Dian Yu, Nan Du, Izhak	755
704	Zhaozhao Xu, Vladimir Braverman, Beidi Chen,	Shafraan, Karthik Narasimhan, and Yuan Cao. 2022.	756
705	and Xia Hu. 2024b. Kivi: A tuning-free asymmetric	React: Synergizing reasoning and acting in language	757
706	2bit quantization for kv cache. <i>arXiv preprint</i>	models. <i>arXiv preprint arXiv:2210.03629</i> .	758
707	<i>arXiv:2402.02750</i> .		
708	MistralAI. 2023. <a href="#">Mistral large 2407: A new milestone</a>	Tianyi Zhang, Faisal Ladhak, Esin Durmus, Percy Liang,	759
709	<a href="#">in open-source language models</a> . Accessed: 2025-	Kathleen McKeown, and Tatsunori B Hashimoto.	760
710	01-21.	2024a. Benchmarking large language models for	761
711	Pavlo Molchanov, Stephen Tyree, Tero Karras, Timo	news summarization. <i>Transactions of the Associa-</i>	762
712	Aila, and Jan Kautz. 2016. Pruning convolutional	<i>tion for Computational Linguistics</i> , 12:39–57.	763
713	neural networks for resource efficient inference.		
714	<i>arXiv preprint arXiv:1611.06440</i> .	Xinrong Zhang, Yingfa Chen, Shengding Hu, Zi-	764
715	Matanel Oren, Michael Hassid, Nir Yarden, Yossi Adi,	hang Xu, Junhao Chen, Moo Khai Hao, Xu Han,	765
716	and Roy Schwartz. 2024. Transformers are multi-	Zhen Leng Thai, Shuo Wang, Zhiyuan Liu, and 1	766
717	state rnns. <i>arXiv preprint arXiv:2401.06104</i> .	others. 2024b. inftybench: Extending long context	767
718	Baptiste Roziere, Jonas Gehring, Fabian Gloeckle, Sten	evaluation beyond 100k tokens. In <i>ACL (1)</i> .	768
719	Sootla, Itai Gat, Xiaoqing Ellen Tan, Yossi Adi,	Zhenyu Zhang, Ying Sheng, Tianyi Zhou, Tianlong	769
720	Jingyu Liu, Romain Sauvestre, Tal Remez, and 1	Chen, Lianmin Zheng, Ruisi Cai, Zhao Song, Yuan-	770
721	others. 2023. Code llama: Open foundation models	dong Tian, Christopher R�, Clark Barrett, and 1 oth-	771
722	for code. <i>arXiv preprint arXiv:2308.12950</i> .	ers. 2023. H2o: Heavy-hitter oracle for efficient	772
		generative inference of large language models. <i>Ad-</i>	773
		<i>vances in Neural Information Processing Systems</i> ,	774
		36:34661–34710.	775

776 Xiabin Zhou, Wenbin Wang, Minyan Zeng, Jiaxian Guo,  
777 Xuebo Liu, Li Shen, Min Zhang, and Liang Ding.  
778 2024. Dynamickv: Task-aware adaptive kv cache  
779 compression for long context llms. *arXiv preprint*  
780 *arXiv:2412.14838*.

## A Derivation and Analysis of the Output Reconstruction Indicator

We define the eviction indicator  $\mathbf{I}_t[n]$  as the reconstruction error of the MHA output caused by removing the  $n$ -th KV pair. Specifically, the eviction indicator is given by:

$$\mathbf{I}_t[n] = \left\| \text{MHA}(\mathbf{x}_t, \langle \mathbf{K}_T, \mathbf{V}_T \rangle) - \text{MHA}(\mathbf{x}_t, \langle \mathbf{K}_{T, \setminus n}, \mathbf{V}_{T, \setminus n} \rangle) \right\|_2, \quad (15)$$

where  $\mathbf{K}_{t, \setminus n}$  and  $\mathbf{V}_{t, \setminus n}$  represent the set of cache keys and values with the  $n$ -th KV pair removed.

Using Eq. (3) and Eq. (4), we can expand Eq. (15) as follows:

$$\mathbf{I}_t[n] = \left\| \mathbf{A}_t \mathbf{V}_T \mathbf{W}_O - \mathbf{A}_{t, \setminus n} \mathbf{V}_{T, \setminus n} \mathbf{W}_O \right\|_2 \quad (16)$$

where  $\mathbf{A}_{t, \setminus n}$  represents the attention weights with the  $n$ -th KV pair removed, and  $\mathbf{V}_{T, \setminus n}$  represents the values corresponding to the remaining cache sets after the removal of the  $n$ -th KV pair.

Further, we expand the matrix computation into a weighted sum form as:

$$\mathbf{I}_t[n] = \left\| \sum_m \mathbf{A}_t[m] \mathbf{v}_m \mathbf{W}_O - \sum_{m \neq n} \mathbf{A}_{t, \setminus n}[m] \mathbf{v}_m \mathbf{W}_O \right\|_2 \quad (17)$$

where  $\mathbf{A}_t[m]$  and  $\mathbf{A}_{t, \setminus n}[m]$  represent the attention weights for the  $m$ -th query in the presence and absence of the  $n$ -th KV pair, respectively.

Compared to  $\mathbf{A}_t[m]$ ,  $\mathbf{A}_{t, \setminus n}[m]$  is missing the component related to  $\mathbf{k}_n$  in the denominator. Therefore, the relationship between the two is given by:

$$\mathbf{A}_{t, \setminus n}[m] = \frac{\mathbf{A}_t[m]}{1 - \mathbf{A}_t[n]} \quad (18)$$

Substituting Eq. (18) into Eq. (17) and performing step-by-step simplifications, we get:

$$\mathbf{I}_t[n] = \left\| \sum_m \mathbf{A}_t[m] \mathbf{v}_m \mathbf{W}_O - \sum_{m \neq n} \frac{\mathbf{A}_t[m]}{1 - \mathbf{A}_t[n]} \mathbf{v}_m \mathbf{W}_O \right\|_2, \quad (19)$$

$$= \left\| \sum_m \mathbf{A}_t[m] \mathbf{v}_m \mathbf{W}_O - \left( \sum_m \frac{\mathbf{A}_t[m]}{1 - \mathbf{A}_t[n]} \mathbf{v}_m \mathbf{W}_O - \frac{\mathbf{A}_t[n]}{1 - \mathbf{A}_t[n]} \mathbf{v}_n \mathbf{W}_O \right) \right\|_2, \quad (20)$$

$$= \left\| \underbrace{\frac{\mathbf{A}_t[n]}{1 - \mathbf{A}_t[n]} \mathbf{v}_n \mathbf{W}_O}_{\text{the } n\text{-th KV pair removed's loss}} - \underbrace{\sum_m \frac{\mathbf{A}_t[m]}{1 - \mathbf{A}_t[n]} \cdot \mathbf{A}_t[m] \mathbf{v}_m \mathbf{W}_O}_{\text{the increase of other components after removing the } n\text{-th KV pair}} \right\|_2, \quad (21)$$

$$= \frac{\mathbf{A}_t[n]}{1 - \mathbf{A}_t[n]} \cdot \left\| \mathbf{v}_n \mathbf{W}_O - \sum_m \mathbf{A}_t[m] \mathbf{v}_m \mathbf{W}_O \right\|_2, \quad (22)$$

$$= \frac{\mathbf{A}_t[n]}{1 - \mathbf{A}_t[n]} \cdot \left\| \text{MHA}(\mathbf{x}_t, \langle \mathbf{K}_T, \mathbf{V}_T \rangle) - \mathbf{v}_n \mathbf{W}_O \right\|_2, \quad (23)$$

From Eq. (21), we can see that the layer-wise output reconstruction indicator can be divided into two parts. One part is the loss due to the removal of the  $n$ -th KV pair, and the other part is the increase in the contribution of the other components after removing the  $n$ -th KV pair. Together, these two parts determine the importance of a KV pair.



## B More Implementation Details

In this section, we provide additional details regarding the implementation of ReST-KV. Our method operates in two main phases: *prompt prefilling* and *token decoding*. During the prompt prefilling stage, we employ Eq. (13) from Section 3.3 as the eviction indicator. This formula integrates both the layer-wise output reconstruction indicator and spatial-temporal smoothing. According to Eq. (14), we select a set of KV pairs based on the cache budget from the prompt. Specifically, for the Exponential Moving Average (EMA) Temporal Smoothing, the smoothing factor  $\alpha$  is set to 0.3. In the case of the Adaptive Window-Based Spatial Smoothing, the scaling factor  $\beta$  is set to 2000. Following SnapKV (Li et al., 2024b), we adopt a fixed observation window of size  $S_w = 32$  and kernel size  $k = 5$  for SnapKV, PyramidKV, and our proposed ReST-KV. To better capture important information, we set the kernel size to 21 on the RULER and InfiniteBench datasets. The StreamingLLM method retains the first 4 tokens as an attention sink, ensuring efficient processing within the token flow. In the token decoding phase, we utilize the KV cache compressed during the prefilling stage, along with a newly updated KV cache, to perform decoding. Notably, no further compression is applied during this phase.

## C Compatibility with Budget Allocation Strategies

In this section, we evaluate the compatibility of our method with existing budget allocation strategies. Specifically, we choose PyramidKV (Cai et al., 2024) as a representative of layer-wise budget allocation strategies and AdaKV (Feng et al., 2024) as a representative of head-wise budget allocation strategies. We compared the average accuracy results of the Llama2-7B-Chat model on the LongBench datasets under varying total cache budgets (ranging from  $64L$  to  $1024L$ ). Our experiments demonstrate that, when combined with these strategies, our method achieves similar or slightly improved performance compared to SnapKV combined with the same strategies.

Table 4: Performance comparison of SnapKV and our method with Pyramid layer-wise budget allocation strategies across varying cache budgets.

Method	Cache Budget $B_{\text{total}}$					Avg. Acc
	$64L$	$128L$	$256L$	$512L$	$1024L$	
SnapKV	22.96	28.31	30.90	32.18	32.99	29.47
PyramidKV	24.67	29.58	31.04	32.32	32.95	30.11 ( $\uparrow$ 0.64%)
ReST-KV	25.54	29.99	31.51	32.38	32.97	30.48
ReST-KV w. Pyramid	<b>26.88</b>	<b>30.47</b>	<b>31.74</b>	<b>32.48</b>	<b>33.05</b>	<b>30.93</b> ( $\uparrow$ 0.45%)

Table 4 illustrates the results of applying Pyramid layer-wise budget allocation strategies to both SnapKV and our method, comparing the performance differences before and after the addition of the strategy. As shown, the accuracy improvements are modest but consistent across different cache budget sizes. For instance, our method combined with layer-wise budget allocation strategies achieves a 0.45% increase in average accuracy across different cache budgets.

Table 5: Performance comparison of SnapKV and our method with Ada head-wise budget allocation strategies across varying cache budgets.

Method	Cache Budget $B_{\text{total}}$					Avg. Acc
	$64L$	$128L$	$256L$	$512L$	$1024L$	
SnapKV	22.96	28.31	30.90	32.18	32.99	29.47
Ada-SnapKV	24.89	29.93	31.21	32.28	33.01	30.26 ( $\uparrow$ 0.79%)
ReST-KV	25.54	29.99	31.51	32.38	32.97	30.48
Ada-ReST-KV	<b>27.35</b>	<b>31.27</b>	<b>31.84</b>	<b>32.51</b>	<b>33.02</b>	<b>31.20</b> ( $\uparrow$ 0.72%)

Table 5 presents the results of applying head-wise budget allocation strategies to both SnapKV and our method, comparing the performance differences before and after the addition of the strategy. The results show that our method combined with AdaKV achieves a 0.72% increase in average accuracy across all

Table 6: Performance comparison across 16 datasets of LongBench on Llama3.1-8B-Instruct for cache budgets from 64L to 1024L. The best result is highlighted in **bold**, and the second-best is underlined.

Method	Single-Document QA			Multi-Document QA			Summarization			Few-shot Learning			Synthetic		Code		Avg.
	NrrvQA	Qasper	MF-en	HotpotQA	2WikiMQA	Musique	GovReport	QMSum	MultiNews	TREC	TriviaQA	SAMSum	PCount	PRE	Lcc	RB-P	
Llama3.1-8B-Instruct, $B_{\text{total}} = Full$																	
Full	32.02	13.12	27.52	16.60	16.41	11.41	34.59	23.41	26.89	73.00	91.65	43.80	7.18	97.73	65.12	58.89	39.96
Llama3.1-8B-Instruct, $B_{\text{total}} = 64L$																	
StreamingLLM	7.65	5.08	14.14	10.93	12.64	6.86	16.57	18.93	16.30	38.50	83.13	34.65	<b>9.78</b>	<b>96.28</b>	54.16	48.21	29.61
H2O	12.23	5.12	15.12	11.51	10.14	6.23	17.23	19.51	16.79	39.15	81.51	36.12	8.12	95.12	51.25	47.12	29.52
TOVA	18.52	<u>6.12</u>	17.32	12.15	12.51	7.35	16.24	20.41	16.34	38.41	82.61	36.16	8.14	<u>95.23</u>	<u>55.21</u>	47.35	30.63
SnapKV	<u>19.90</u>	5.78	<u>18.38</u>	<u>13.51</u>	<u>14.42</u>	<b>8.52</b>	<u>17.35</u>	<u>20.44</u>	<u>17.33</u>	<u>41.00</u>	<u>85.37</u>	<u>37.63</u>	<u>8.93</u>	91.08	55.09	<b>48.88</b>	<u>31.48</u>
ReST-KV	<b>22.43</b>	<b>7.19</b>	<b>19.25</b>	<b>14.11</b>	<b>15.04</b>	<u>7.97</u>	<b>20.56</b>	<b>21.10</b>	<b>19.15</b>	<b>53.50</b>	<b>88.23</b>	<b>40.21</b>	8.46	93.90	<b>56.74</b>	<u>48.77</u>	<b>33.54</b>
Llama3.1-8B-Instruct, $B_{\text{total}} = 128L$																	
StreamingLLM	16.07	5.34	14.82	11.01	12.38	6.61	17.99	19.06	18.69	40.50	85.57	38.24	<u>9.20</u>	94.11	<u>58.97</u>	49.70	31.14
H2O	14.00	5.45	16.62	12.83	10.87	6.94	17.29	20.88	16.96	40.27	82.15	37.61	9.12	<u>96.13</u>	<u>52.13</u>	48.16	30.46
TOVA	21.63	<u>8.11</u>	18.70	<u>14.31</u>	14.44	<b>9.46</b>	19.22	<b>22.97</b>	17.60	40.76	84.40	39.21	<b>11.24</b>	<b>96.67</b>	58.25	48.91	32.87
SnapKV	<u>25.20</u>	7.23	<u>20.89</u>	13.60	<u>14.61</u>	8.49	20.95	21.42	<u>21.28</u>	<u>48.00</u>	<u>89.38</u>	40.08	7.29	93.78	<b>59.31</b>	<b>52.12</b>	33.98
ReST-KV	<b>27.88</b>	<b>8.29</b>	<b>22.22</b>	<b>14.65</b>	<b>14.70</b>	<u>9.32</u>	<b>22.26</b>	<u>22.95</u>	<b>22.16</b>	<b>65.00</b>	<b>91.03</b>	<b>41.26</b>	8.20	93.59	58.78	<u>51.50</u>	<b>35.86</b>
Llama3.1-8B-Instruct, $B_{\text{total}} = 256L$																	
StreamingLLM	16.03	5.50	14.96	10.38	12.25	7.01	20.38	19.48	20.63	46.00	87.49	41.02	<u>9.57</u>	90.53	61.13	51.44	32.11
H2O	13.99	6.48	17.76	13.41	11.10	7.38	17.64	21.74	18.21	40.29	82.22	38.11	8.90	96.89	51.53	49.14	30.92
TOVA	24.05	<b>11.17</b>	21.30	<b>17.61</b>	<b>17.50</b>	<b>12.84</b>	21.93	<b>26.16</b>	20.58	43.69	87.29	<b>42.52</b>	<b>14.21</b>	<b>99.26</b>	60.92	51.65	35.79
SnapKV	<u>27.83</u>	9.12	<u>22.21</u>	13.68	14.52	<u>10.20</u>	<u>23.02</u>	23.14	<u>22.51</u>	<u>56.50</u>	<u>90.63</u>	40.79	7.89	<u>97.56</u>	<b>62.05</b>	<b>55.47</b>	<u>36.07</u>
ReST-KV	<b>29.14</b>	<u>9.54</u>	<b>23.61</b>	<u>14.27</u>	<u>14.61</u>	9.31	<b>24.32</b>	<u>23.59</u>	<b>23.47</b>	<b>67.00</b>	<b>92.13</b>	<u>42.04</u>	8.09	94.51	<u>61.56</u>	<u>53.62</u>	<b>36.93</b>
Llama3.1-8B-Instruct, $B_{\text{total}} = 512L$																	
StreamingLLM	19.15	6.47	15.02	10.94	12.58	6.23	23.66	20.05	23.31	57.50	87.70	41.86	<b>10.25</b>	90.74	62.39	53.61	33.84
H2O	26.23	7.34	20.51	11.52	13.52	7.34	23.23	21.24	23.14	58.50	86.12	40.15	7.25	91.02	61.23	54.12	34.53
TOVA	27.34	8.34	22.45	12.25	14.51	8.42	24.23	22.13	22.25	58.50	89.31	40.51	8.24	93.14	62.23	55.61	35.59
SnapKV	<u>28.02</u>	<u>9.83</u>	<u>24.84</u>	<u>13.77</u>	<u>15.40</u>	<u>10.21</u>	<u>25.13</u>	<u>22.73</u>	<u>24.25</u>	<u>65.00</u>	<b>92.34</b>	41.69	<u>8.42</u>	<u>96.31</u>	<b>64.30</b>	<b>57.28</b>	<u>37.47</u>
ReST-KV	<b>32.01</b>	<b>10.73</b>	<b>25.23</b>	<b>15.91</b>	<b>15.85</b>	<b>10.25</b>	<b>26.47</b>	<b>23.23</b>	<b>24.79</b>	<b>69.00</b>	<u>91.62</u>	<b>42.59</b>	8.40	<b>97.66</b>	<u>63.48</u>	<u>56.03</u>	<b>38.33</b>
Llama3.1-8B-Instruct, $B_{\text{total}} = 1024L$																	
StreamingLLM	20.50	8.08	15.72	11.61	12.39	6.71	25.76	20.18	25.44	63.50	88.84	42.61	<u>10.03</u>	92.10	63.15	55.88	35.16
H2O	27.63	8.84	21.98	12.99	15.91	8.23	23.96	<u>23.77</u>	24.20	59.79	86.97	41.52	9.07	93.01	63.59	56.08	36.10
TOVA	29.82	9.73	25.10	14.92	<b>17.53</b>	10.20	<u>27.06</u>	23.20	24.78	59.89	<b>92.21</b>	<b>43.49</b>	<b>10.38</b>	95.86	64.08	57.47	37.86
SnapKV	<b>31.95</b>	<u>11.26</u>	<u>25.56</u>	<u>15.13</u>	<u>16.18</u>	<u>10.79</u>	26.97	23.06	<u>25.89</u>	<u>67.50</u>	<u>91.90</u>	<u>42.88</u>	7.67	<b>98.16</b>	<b>64.53</b>	<b>58.30</b>	<u>38.61</u>
ReST-KV	<u>31.83</u>	<b>11.61</b>	<b>26.51</b>	<b>15.85</b>	15.48	<b>10.83</b>	<b>28.20</b>	<b>24.00</b>	<b>26.18</b>	<b>70.50</b>	91.73	42.70	8.02	<u>97.79</u>	<u>64.24</u>	<u>57.56</u>	<b>38.94</b>

cache budgets. These results highlight that our method is compatible with existing budget allocation strategies.

## D Additional Experiments on LongBench

In this section, we provide comprehensive experimental results on LongBench (Bai et al., 2023), a benchmark focused on long-context understanding, with input lengths ranging from 1235 to 18409 tokens. We perform detailed performance evaluations for three base models with cache budgets ranging from 64L to 1024L: Llama2-7B-Chat (Touvron et al., 2023), Llama3.1-8B-Instruct (Dubey et al., 2024), and Mistral-7B-Instruct-v0.3 (Jiang et al., 2023) (Appendix D.1). To demonstrate the generality of ReST-KV, we also conduct experiments across different models and sizes. In Appendix D.2, we report additional experiments on the Qwen2.5-7B-Instruct (Team, 2024) and Gemma-7B-Instruct (Team et al., 2024) model architectures, and in Appendix D.3, we present experiments on the Llama2-13B-Chat and Llama3-70B-Instruct model sizes.

### D.1 Detailed Performance Across Cache Budgets

Tables 6, 7, and 8 present the detailed LongBench results of ReST-KV and comparative methods applied to Llama3.1-8B-Instruct, Mistral-7B-Instruct-v0.3, and Llama2-7B-Chat, respectively. Overall, the results demonstrate that, compared to other methods, ReST-KV consistently outperforms all baselines across all tasks in LongBench when applied to the test models with cache budgets ranging from 64L to 1024L. This proves the effectiveness and wide applicability of ReST-KV in efficient long-context processing using KV caches in open-source LLMs across domains.

Table 7: Performance comparison across 16 datasets of LongBench on Mistral-7B-Instruct-v0.3 for cache budgets from 64L to 1024L. The best result is highlighted in **bold**, and the second-best is underlined.

Method	Single-Document QA			Multi-Document QA			Summarization			Few-shot Learning			Synthetic		Code		Avg.
	NrrvQA	Qasper	MF-en	HotpotQA	2WikiMQA	Musique	GovReport	QMSum	MultiNews	TREC	TriviaQA	SAMSum	PCount	PRE	Lcc	RB-P	
Mistral-7B-Instruct-v0.3, $B_{\text{total}} = Full$																	
Full	29.07	41.54	52.88	49.37	39.01	28.58	35.07	25.71	27.73	76.00	88.59	47.51	6.00	98.50	61.48	62.68	48.11
Mistral-7B-Instruct-v0.3, $B_{\text{total}} = 64L$																	
StreamingLLM	20.37	20.56	24.62	38.87	32.47	17.68	15.48	19.84	15.81	39.50	82.77	36.72	5.50	80.00	49.77	47.90	34.24
H2O	20.51	21.52	25.12	40.12	33.12	18.34	16.23	19.12	16.24	38.50	83.12	37.23	6.00	85.50	50.12	48.12	34.93
TOVA	<u>22.51</u>	22.24	37.23	41.12	34.10	19.52	17.21	19.23	16.27	38.50	85.12	38.51	<u>6.50</u>	<u>86.50</u>	51.04	48.42	36.50
SnapKV	19.39	<u>23.62</u>	<u>38.66</u>	<u>43.26</u>	<u>34.72</u>	<u>21.33</u>	<u>17.59</u>	<u>20.93</u>	<u>17.06</u>	38.50	<u>86.96</u>	<u>39.61</u>	<b>7.00</b>	<b>90.50</b>	<u>51.63</u>	<u>49.73</u>	<u>37.53</u>
ReST-KV	<b>25.65</b>	<b>26.58</b>	<b>42.71</b>	<b>46.11</b>	<b>36.43</b>	<b>24.34</b>	<b>19.80</b>	<b>21.65</b>	<b>18.90</b>	<b>51.50</b>	<b>87.88</b>	<b>41.54</b>	4.00	<b>90.50</b>	<b>52.39</b>	<b>50.75</b>	<b>40.05</b>
Mistral-7B-Instruct-v0.3, $B_{\text{total}} = 128L$																	
StreamingLLM	21.39	22.05	26.73	37.25	32.81	17.61	16.76	19.69	17.98	<u>45.50</u>	85.64	40.49	<u>5.50</u>	80.00	55.01	52.12	36.03
H2O	22.39	22.98	26.92	42.51	33.19	19.20	16.90	20.70	16.82	41.12	87.10	39.76	<b>8.58</b>	86.19	50.81	53.01	36.76
TOVA	22.48	<u>28.78</u>	<u>48.71</u>	<b>47.58</b>	34.26	21.96	<u>21.67</u>	21.75	<u>21.68</u>	42.23	87.04	42.10	2.08	94.58	<b>56.97</b>	54.76	40.54
SnapKV	<u>25.04</u>	<u>28.42</u>	47.88	46.23	<u>36.47</u>	<u>24.60</u>	21.22	<b>22.74</b>	21.15	45.00	<b>88.74</b>	<u>43.07</u>	4.00	<u>95.00</u>	<u>56.81</u>	<b>55.75</b>	<u>41.38</u>
ReST-KV	<b>26.58</b>	<b>29.60</b>	<b>49.23</b>	<u>47.46</u>	<b>37.18</b>	<b>25.16</b>	<b>22.44</b>	<u>22.43</u>	<b>21.77</b>	<b>69.00</b>	<u>88.18</u>	<b>43.84</b>	<u>5.50</u>	<b>96.50</b>	56.29	<u>55.13</u>	<b>43.52</b>
Mistral-7B-Instruct-v0.3, $B_{\text{total}} = 256L$																	
StreamingLLM	22.46	23.32	29.63	39.62	32.01	16.71	19.13	19.30	20.14	54.50	85.12	43.21	<u>5.50</u>	80.00	57.72	55.03	37.71
H2O	24.31	23.78	27.97	43.90	33.95	19.87	17.42	<u>23.36</u>	17.32	43.74	<b>91.10</b>	40.17	<b>11.88</b>	86.92	51.54	54.24	38.22
TOVA	<b>28.17</b>	29.93	51.01	46.26	36.55	26.65	22.76	22.31	21.24	54.34	88.00	42.45	2.16	<u>94.49</u>	57.39	58.04	42.61
SnapKV	26.88	<u>31.72</u>	<u>51.40</u>	<b>48.89</b>	<u>36.80</u>	<b>27.33</b>	<u>22.85</u>	<b>23.66</b>	<u>23.15</u>	<u>57.00</u>	<u>89.01</u>	<u>43.60</u>	5.00	<b>96.50</b>	<b>58.64</b>	<u>58.21</u>	<u>43.79</u>
ReST-KV	<u>27.43</u>	<b>34.24</b>	<b>52.11</b>	<u>48.81</u>	<b>38.25</b>	<u>27.20</u>	<b>24.31</b>	23.33	<b>23.24</b>	<b>72.50</b>	88.59	<b>44.61</b>	<u>5.50</u>	<b>96.50</b>	<u>58.41</u>	<b>59.21</b>	<b>45.27</b>
Mistral-7B-Instruct-v0.3, $B_{\text{total}} = 512L$																	
StreamingLLM	24.19	25.97	30.14	40.75	31.90	17.35	22.18	20.30	23.22	65.50	86.95	43.75	<b>6.00</b>	81.00	59.35	56.36	39.68
H2O	25.23	30.41	40.32	42.52	35.23	18.23	24.23	21.24	23.21	66.50	86.71	43.15	5.00	82.52	<u>60.13</u>	58.15	41.42
TOVA	25.23	32.52	46.24	45.23	36.23	20.32	24.53	22.53	23.64	66.50	87.24	44.21	<b>6.00</b>	<u>85.62</u>	59.35	60.24	42.85
SnapKV	<u>26.84</u>	<u>35.51</u>	<u>53.12</u>	<b>49.56</b>	<u>37.72</u>	<u>26.54</u>	<u>25.06</u>	<u>24.03</u>	<u>24.76</u>	<u>67.50</u>	<u>89.36</u>	<u>44.82</u>	<u>5.50</u>	<b>98.50</b>	<b>60.44</b>	<b>61.22</b>	<u>45.66</u>
ReST-KV	<b>28.60</b>	<b>35.86</b>	<b>53.37</b>	<u>49.13</u>	<b>38.70</b>	<b>27.94</b>	<b>26.05</b>	<b>24.37</b>	<b>25.09</b>	<b>73.50</b>	<b>89.66</b>	<b>46.27</b>	<u>5.50</u>	<b>98.50</b>	<u>60.13</u>	<u>60.84</u>	<b>46.47</b>
Mistral-7B-Instruct-v0.3, $B_{\text{total}} = 1024L$																	
StreamingLLM	24.81	27.98	31.09	42.93	32.65	18.03	24.57	20.74	25.42	68.50	88.71	45.37	<u>5.50</u>	82.50	61.07	59.21	41.19
H2O	28.23	32.61	42.96	45.03	38.39	20.56	26.50	24.01	25.10	69.37	88.49	45.60	<b>8.11</b>	83.81	<b>62.79</b>	59.90	43.84
TOVA	29.10	36.82	<b>53.78</b>	<u>49.25</u>	38.39	<u>28.33</u>	<u>27.17</u>	23.75	25.53	70.39	88.28	45.24	4.85	<b>100.47</b>	60.40	<b>62.25</b>	46.50
SnapKV	<b>29.31</b>	<u>37.25</u>	<u>53.55</u>	<u>49.25</u>	<u>38.54</u>	<u>28.28</u>	26.90	24.49	26.27	<u>72.50</u>	<u>89.11</u>	<u>46.08</u>	<u>5.50</u>	99.00	61.45	61.76	46.83
ReST-KV	<u>29.20</u>	<b>37.72</b>	52.56	<b>50.50</b>	<b>38.89</b>	<b>28.69</b>	<b>28.03</b>	<b>24.71</b>	<b>26.76</b>	<b>74.00</b>	<b>89.41</b>	<b>47.08</b>	<u>5.50</u>	<u>99.00</u>	61.10	61.66	<b>47.18</b>

## D.2 Additional Experiments on More Model Architectures

To further validate the versatility of ReST-KV across different model architectures, we performed additional experiments on the Qwen2.5-7B-Instruct and Gemma-7B-Instruct models. The experiments were conducted in two distinct memory configurations: a low-memory setting ( $B_{\text{total}} = 64L$ ) and a high-memory setting ( $B_{\text{total}} = 512L$ ). As shown in Table 9, ReST-KV consistently outperforms baseline methods in both the low and high memory settings for the Qwen and Gemma architectures, similar to the results observed with the Llama and Mistral models. These findings further confirm the adaptability of ReST-KV across various model architectures, demonstrating its robust performance advantage regardless of the underlying design of the models.

## D.3 Additional Experiments on Larger-scale Models

To assess the scalability of ReST-KV on larger models, we conducted additional experiments on Llama2-13B-Chat and Llama3-70B-Instruct. These experiments were performed under two different memory configurations: a low-memory setting ( $B_{\text{total}} = 64L$ ) and a high-memory setting ( $B_{\text{total}} = 512L$ ). As shown in Table 10, ReST-KV consistently outperforms baseline methods in both low and high memory settings for the Llama2-13B-Chat and Llama3-70B-Instruct models. These results further demonstrate the scalability and effectiveness of ReST-KV when applied to larger-scale models, highlighting its continued performance advantage regardless of the model size.

Table 8: Performance comparison across 16 datasets of LongBench on Llama2-7B-Chat for cache budgets from 64L to 1024. The best result is highlighted in **bold**, and the second-best is underlined.

Method	Single-Document QA			Multi-Document QA			Summarization			Few-shot Learning			Synthetic		Code		Avg.
	NrrvQA	Qasper	MF-en	HotpotQA	2WikiMQA	Musique	GovReport	QMSum	MultiNews	TREC	TriviaQA	SAMSum	PCount	PRE	Lcc	RB-P	
Llama2-7B-Chat, $B_{\text{total}} = Full$																	
Full	18.39	20.11	35.67	31.25	25.50	10.14	25.68	20.93	26.27	64.00	83.38	40.99	5.50	10.00	60.81	55.27	33.37
Llama2-7B-Chat, $B_{\text{total}} = 64L$																	
StreamingLLM	5.61	15.51	6.42	14.14	16.77	1.36	12.09	16.46	12.83	17.25	15.12	10.93	<u>4.50</u>	3.00	22.00	15.24	11.83
H2O	4.46	12.14	8.85	12.11	13.34	2.36	13.06	16.63	<u>16.89</u>	19.50	20.69	10.45	2.70	3.00	26.50	16.06	12.42
TOVA	8.26	14.34	12.64	13.52	13.25	3.53	11.64	16.67	13.35	<u>36.00</u>	<u>72.64</u>	32.72	2.00	<u>4.00</u>	36.15	32.53	20.20
SnapKV	<u>10.83</u>	<u>16.38</u>	<u>17.53</u>	<u>22.81</u>	<u>23.24</u>	<u>5.06</u>	<u>13.12</u>	<u>18.38</u>	14.17	34.50	69.45	<b>33.43</b>	<b>5.50</b>	<b>7.00</b>	<u>39.99</u>	<u>36.04</u>	<u>22.96</u>
ReST-KV	<b>12.72</b>	<b>17.17</b>	<b>24.09</b>	<b>24.71</b>	<b>23.80</b>	<b>5.55</b>	<b>15.18</b>	<b>19.71</b>	<b>17.45</b>	<b>43.50</b>	<b>76.17</b>	<u>33.42</u>	<b>5.50</b>	<u>4.00</u>	<b>45.00</b>	<b>40.61</b>	<b>25.54</b>
Llama2-7B-Chat, $B_{\text{total}} = 128L$																	
StreamingLLM	8.45	14.87	12.68	19.98	22.14	5.17	13.99	<u>19.74</u>	16.02	28.50	60.96	30.61	5.00	5.00	44.44	39.53	21.69
H2O	7.60	9.53	9.92	18.35	15.64	3.30	<u>17.75</u>	14.71	<b>21.45</b>	28.00	39.61	13.85	4.17	3.56	29.92	25.53	16.43
TOVA	12.26	14.66	25.72	26.08	24.21	6.90	15.28	18.30	17.61	42.44	80.12	35.25	<u>5.05</u>	6.93	52.48	49.17	27.03
SnapKV	<u>13.32</u>	<u>16.28</u>	<u>27.23</u>	<u>27.23</u>	<u>24.37</u>	<u>7.17</u>	<u>16.97</u>	<u>19.65</u>	<u>19.38</u>	<u>44.00</u>	<u>81.88</u>	<u>36.82</u>	<b>6.00</b>	<b>8.00</b>	<b>54.02</b>	<b>50.66</b>	<u>28.31</u>
ReST-KV	<b>15.55</b>	<b>17.78</b>	<b>27.24</b>	<b>27.72</b>	<b>24.62</b>	<b>8.93</b>	<b>17.88</b>	<b>20.13</b>	<u>20.92</u>	<b>60.00</b>	<b>82.48</b>	<b>37.35</b>	<b>6.00</b>	<b>9.50</b>	<u>53.45</u>	<u>50.24</u>	<b>29.99</b>
Llama2-7B-Chat, $B_{\text{total}} = 256L$																	
StreamingLLM	13.81	15.51	17.63	25.81	24.48	7.70	16.16	19.33	18.78	44.00	78.87	37.63	<u>5.50</u>	5.00	54.57	49.68	27.15
H2O	8.82	11.73	10.11	15.54	13.70	3.78	<b>19.29</b>	19.13	<b>23.36</b>	34.00	35.61	20.26	4.75	3.57	23.74	23.75	16.95
TOVA	14.12	16.82	29.15	27.69	24.82	6.89	18.04	18.67	21.79	57.01	<u>83.48</u>	37.74	5.06	8.71	56.51	<u>52.99</u>	29.97
SnapKV	<b>15.45</b>	<u>17.57</u>	<u>29.44</u>	<u>29.53</u>	<u>24.94</u>	<u>8.69</u>	18.78	<u>20.48</u>	<u>22.15</u>	<u>57.50</u>	<b>83.76</b>	<u>38.25</u>	<b>6.00</b>	<u>10.50</u>	<b>57.75</b>	<b>53.59</b>	<u>30.90</u>
ReST-KV	<u>15.23</u>	<b>18.57</b>	<b>30.46</b>	<b>31.53</b>	<b>25.85</b>	<b>9.09</b>	<u>19.13</u>	<b>20.83</b>	<u>22.28</u>	<b>63.00</b>	82.57	<b>39.05</b>	<b>6.00</b>	<b>11.50</b>	<u>57.16</u>	51.91	<b>31.51</b>
Llama2-7B-Chat, $B_{\text{total}} = 512L$																	
StreamingLLM	15.30	15.53	20.16	26.59	25.05	5.65	18.30	19.28	21.84	54.50	82.23	38.07	<u>5.50</u>	5.00	56.80	51.95	28.86
H2O	9.68	8.67	6.86	10.85	8.71	1.31	20.04	18.72	<b>24.91</b>	18.00	17.09	18.99	3.75	2.30	20.87	14.87	12.85
TOVA	13.53	15.46	26.44	26.12	<b>31.02</b>	7.12	18.25	18.64	22.34	<u>62.50</u>	<u>83.10</u>	<b>40.61</b>	3.00	8.00	56.14	51.53	30.24
SnapKV	<u>16.22</u>	<u>19.57</u>	<u>32.32</u>	<u>31.87</u>	24.97	<u>9.66</u>	<u>20.19</u>	<b>20.77</b>	<u>23.85</u>	62.00	82.24	39.18	<b>6.00</b>	<u>10.50</u>	<b>59.49</b>	<b>56.06</b>	<u>32.18</u>
ReST-KV	<b>17.15</b>	<b>19.88</b>	<b>32.71</b>	<b>31.94</b>	<u>25.62</u>	<b>9.97</b>	<b>20.52</b>	<u>20.68</u>	23.59	<b>63.50</b>	<b>83.30</b>	<u>39.29</u>	<b>6.00</b>	<b>11.50</b>	<u>58.65</u>	<u>53.81</u>	<b>32.38</b>
Llama2-7B-Chat, $B_{\text{total}} = 1024L$																	
StreamingLLM	15.12	17.35	22.21	26.76	24.43	6.52	21.15	19.16	24.67	61.00	82.16	39.69	<b>6.00</b>	1.50	57.73	53.24	29.92
H2O	6.55	11.17	8.96	13.56	9.57	1.80	<u>22.43</u>	19.74	<u>26.07</u>	18.50	15.59	36.61	4.43	1.08	29.96	15.24	15.08
TOVA	16.84	19.32	34.90	31.07	25.24	9.51	20.36	20.34	23.42	62.38	81.31	39.68	4.03	<u>10.05</u>	58.13	54.73	31.96
SnapKV	<u>17.41</u>	19.74	<b>35.92</b>	<b>31.82</b>	<b>26.00</b>	<u>10.09</u>	22.06	20.43	24.88	<u>63.50</u>	82.77	40.52	<b>6.00</b>	<b>10.50</b>	60.10	<b>56.05</b>	<b>32.99</b>
ReST-KV	17.39	<u>20.01</u>	35.33	<u>31.71</u>	25.33	9.60	22.30	<u>20.85</u>	24.91	<u>63.50</u>	<b>83.73</b>	<u>40.76</u>	<b>6.00</b>	<b>10.50</b>	<u>60.57</u>	54.95	<u>32.97</u>

## E Additional Experiments on RULER Benchmark

In this section, we present a detailed evaluation of ReST-KV on the various subtasks of the RULER benchmark (Hsieh et al., 2024). RULER is specifically designed to assess the core capabilities of LLMs in long-context scenarios through a diverse suite of tasks.

The retrieval suite includes four variants of the needle-in-a-haystack (NIAH) test—Single-Needle (S-NIAH), Multi-Key (MK-NIAH), Multi-Query (MQ-NIAH), and Multi-Value (MV-NIAH)—to evaluate recall accuracy under diverse distractor settings and query formulations. Beyond retrieval, the Variable Tracking (VT) task measures multi-hop reasoning by requiring models to resolve transitive variable references scattered throughout the input. Lastly, aggregation tasks such as Common Word Extraction (CWE) and Frequent Word Extraction (FWE) test a model’s ability to compress and synthesize high-density signal distributed across long contexts. These tasks collectively pose distinct challenges for context retention, salience estimation, and compositional reasoning, providing a holistic benchmark for evaluating memory management strategies like ReST-KV.

We evaluate ReST-KV using the LLaMA-3.1-8B-Instruct model with a maximum context window of  $B = 1024L$ , across input lengths ranging from 4k to 128k tokens. The evaluation compares ReST-KV with several representative KV cache eviction baselines: Full KV cache (oracle), StreamingLLM (Xiao et al., 2023), SnapKV (Li et al., 2024b), and PyramidKV (Cai et al., 2024).

As reported in Table 11, ReST-KV consistently achieves higher average accuracy than all alternative eviction strategies across all context lengths. For instance, at 4k tokens, ReST-KV achieves an average accuracy of 94.01%, substantially outperforming SnapKV (83.60%) and PyramidKV (85.21%). While all



Table 9: Performance comparison across 16 datasets of LongBench on Qwen2.5-7B-Instruct and Gemma-7B-Instruct. The best result is highlighted in **bold**, and the second-best is underlined.

Method	Single-Document QA			Multi-Document QA			Summarization			Few-shot Learning			Synthetic		Code		Avg.
	NrrvQA	Qasper	MF-en	HotpotQA	2WikiMQA	Musique	GovReport	QMSum	MultiNews	TREC	TriviaQA	SAMSum	PCount	PRE	Lcc	RB-P	
Qwen2.5-7B-Instruct, $B_{\text{total}} = \text{Full}$																	
Full	3.82	10.75	24.24	10.23	9.30	6.97	32.54	17.84	22.46	71.50	89.32	46.16	4.35	98.83	61.93	68.2	36.15
Qwen2.5-7B-Instruct, $B_{\text{total}} = 64L$																	
StreamingLLM	2.74	5.53	13.16	7.62	7.70	4.35	14.98	12.70	11.96	38.50	77.44	37.51	6.29	26.29	44.14	44.40	22.21
H2O	1.09	3.46	17.22	6.57	6.33	4.23	14.50	11.67	10.29	37.38	76.86	37.81	7.76	83.84	46.11	49.59	25.92
TOVA	2.19	3.58	17.34	8.23	8.14	5.96	16.48	13.38	11.36	37.94	78.75	39.12	7.79	85.47	47.93	50.24	27.12
SnapKV	2.86	5.58	18.71	8.59	8.41	6.01	16.96	13.67	13.21	39.50	79.09	40.39	7.92	87.02	48.10	51.52	27.97
ReST-KV	3.27	6.69	18.95	9.57	8.79	6.03	18.77	14.99	15.19	50.50	79.07	41.28	4.73	93.00	48.47	50.03	29.33
Qwen2.5-7B-Instruct, $B_{\text{total}} = 512L$																	
StreamingLLM	2.98	6.70	15.29	8.28	8.27	4.15	22.54	13.15	18.90	56.00	85.96	43.43	6.84	36.21	54.08	53.69	27.28
H2O	1.16	6.46	21.50	8.05	8.50	6.00	23.09	15.25	17.63	63.65	81.84	43.52	2.03	93.33	57.68	61.67	31.96
TOVA	2.70	7.99	21.77	8.61	8.57	6.61	23.44	16.34	19.42	64.28	82.98	44.41	2.35	94.70	59.23	63.58	32.94
SnapKV	3.57	8.90	22.88	10.34	9.57	6.74	24.73	17.58	19.56	64.50	83.49	45.08	4.32	96.67	59.93	64.54	33.90
ReST-KV	3.53	9.46	23.66	10.91	9.76	7.24	25.65	17.76	20.23	67.50	86.73	44.93	3.83	98.08	60.14	63.56	34.56
Gemma-7B-Instruct, $B_{\text{total}} = \text{Full}$																	
Full	14.28	33.12	41.08	30.75	26.11	15.47	23.95	19.31	23.86	69.50	81.28	36.22	4.00	35.92	48.47	48.79	34.51
Gemma-7B-Instruct, $B_{\text{total}} = 64L$																	
StreamingLLM	11.31	16.54	22.96	21.87	23.25	10.18	12.47	16.80	12.74	38.50	70.94	29.79	2.50	20.50	44.67	48.75	25.24
H2O	10.37	15.93	33.33	26.09	23.65	12.52	12.49	16.94	12.99	39.15	80.42	32.23	3.20	24.41	46.00	49.03	27.42
TOVA	10.53	16.58	33.81	27.05	24.56	12.66	13.26	17.19	13.76	39.68	80.69	32.67	3.68	25.29	46.01	49.94	27.96
SnapKV	11.05	17.06	34.22	27.41	25.32	13.52	13.98	17.35	14.03	40.50	81.42	32.90	3.83	26.00	46.34	49.95	28.43
ReST-KV	13.10	22.90	36.78	28.36	25.90	15.13	15.39	18.09	15.68	44.50	82.55	32.77	3.33	36.25	47.92	48.70	30.46
Gemma-7B-Instruct, $B_{\text{total}} = 512L$																	
StreamingLLM	11.58	20.76	26.09	24.06	23.36	10.62	17.49	17.01	20.12	60.50	78.20	37.45	1.83	25.17	49.88	52.64	29.80
H2O	12.70	29.01	38.66	28.71	25.10	14.19	17.53	17.70	20.09	60.94	80.75	35.24	3.15	34.02	47.44	49.01	32.14
TOVA	13.23	29.30	39.32	29.63	25.57	14.55	18.12	18.32	21.01	61.13	81.49	35.78	3.61	34.46	48.39	50.00	32.74
SnapKV	13.36	29.43	39.80	30.24	26.01	14.82	18.30	18.86	21.23	62.00	81.51	36.04	4.33	35.08	49.16	50.73	33.18
ReST-KV	13.70	30.33	42.08	30.13	26.06	14.37	18.82	18.60	22.38	69.00	81.72	37.55	4.33	35.21	48.67	49.48	33.90

methods exhibit declining performance as the context length increases, ReST-KV maintains a clear and consistent margin over the baselines, demonstrating its robustness in extended-context scenarios.

A breakdown by task category reveals that ReST-KV performs particularly well on retrieval tasks (S-NIAH, MQ-NIAH, MV-NIAH) and multi-hop reasoning (VT), often approaching the accuracy levels of the full KV cache. These results indicate that ReST-KV is effective at preserving semantically salient tokens under constrained memory. More challenging tasks, such as MK-NIAH-3 and the CWE aggregation task with uniform word distributions, remain difficult across all methods. Nonetheless, ReST-KV continues to outperform other eviction baselines in these settings, suggesting stronger resilience to task complexity and noise.

## F Additional Experiments on Needle-in-a-Haystack Test

In this section, we present additional experiments to further evaluate the effectiveness of our method on the Needle-in-a-Haystack test. This benchmark assesses a model’s ability to retrieve critical information embedded within long contexts. While Section 4.4 already provides results for Mistral-7B-Instruct-v0.3 with a cache budget of  $B = 1024L$ , we extend our analysis by considering additional settings: (1) Mistral-7B-Instruct-v0.3 with a reduced cache budget of  $B = 128L$ , (2) Llama3.1-8B-Instruct under both  $B = 128L$  and  $B = 1024L$ .

Figures 7, 8 and 9 illustrate the performance comparison under these settings. We observe the following key insights:

- **Mistral-7B-Instruct-v0.3** ( $B = 128L$ ) retains **76%** of the original accuracy, outperforming SnapKV by **14%**. This demonstrates that our method maintains strong retrieval capability even under severe cache constraints.
- **Llama3.1-8B-Instruct** ( $B = 128L$ ) achieves **74%** accuracy, surpassing SnapKV by **6%**, indicating its robustness in preserving key-value pairs under limited cache budgets.

Table 10: Performance comparison across 16 datasets of LongBench on Llama models from 13B to 70B. The best result is highlighted in **bold**, and the second-best is underlined.

Method	Single-Document QA			Multi-Document QA			Summarization			Few-shot Learning			Synthetic		Code		Avg.
	NrrvQA	Qasper	MF-en	HotpotQA	2WikiMQA	Musique	GovReport	QMSum	MultiNews	TREC	TriviaQA	SAMSum	PCount	PRE	Lcc	RB-P	
Llama2-13B-Chat, $B_{\text{total}} = Full$																	
Full	19.19	25.86	37.04	36.65	33.22	14.02	25.92	20.24	26.02	65.00	87.70	35.60	3.60	11.00	51.26	53.15	34.09
Llama2-13B-Chat, $B_{\text{total}} = 64L$																	
StreamingLLM	6.95	15.50	16.08	24.30	26.66	7.49	0.98	17.89	2.17	29.50	55.63	16.70	3.00	5.50	34.05	29.27	18.23
H2O	14.00	<u>18.17</u>	21.78	30.62	<u>28.77</u>	9.93	14.88	<u>19.17</u>	<u>17.97</u>	<u>35.00</u>	80.11	28.97	<b>3.87</b>	6.50	37.50	30.11	24.83
TOVA	<u>15.10</u>	17.12	24.22	34.11	28.32	10.69	14.60	18.89	16.83	33.57	<u>86.42</u>	29.99	3.13	9.79	<u>40.48</u>	38.05	26.33
SnapKV	<b>16.05</b>	<u>17.20</u>	<u>24.85</u>	<u>34.51</u>	28.72	<b>11.52</b>	<u>15.39</u>	<b>19.34</b>	16.89	34.50	<b>86.87</b>	<b>30.94</b>	<u>3.54</u>	<u>10.00</u>	<b>40.65</b>	<u>38.22</u>	<u>26.82</u>
ReST-KV	14.97	<b>20.02</b>	<b>32.61</b>	<b>35.27</b>	<b>29.15</b>	<u>10.71</u>	<b>17.21</b>	19.12	<b>18.39</b>	<b>42.00</b>	85.35	<u>30.57</u>	<u>3.54</u>	<b>12.00</b>	40.01	<b>41.41</b>	<b>28.27</b>
Llama2-13B-Chat, $B_{\text{total}} = 512L$																	
StreamingLLM	14.80	19.01	21.58	33.08	28.92	12.43	20.27	18.27	19.82	56.50	<u>85.98</u>	33.02	<u>4.05</u>	7.50	49.21	47.83	29.52
H2O	17.28	20.94	27.81	32.98	29.39	10.66	<b>21.57</b>	19.50	<b>24.49</b>	61.50	82.61	34.51	<b>4.34</b>	9.50	47.58	45.41	30.63
TOVA	16.95	21.97	33.18	35.51	31.11	13.94	20.33	19.74	22.94	62.33	85.54	<u>35.06</u>	2.94	<u>10.57</u>	49.60	49.80	31.97
SnapKV	17.46	<u>22.46</u>	<u>33.79</u>	<b>36.39</b>	<u>31.37</u>	<u>14.46</u>	20.51	<u>19.81</u>	23.76	<u>62.50</u>	<u>85.98</u>	<b>35.88</b>	3.55	<b>11.50</b>	<b>50.12</b>	50.08	32.48
ReST-KV	<b>18.00</b>	<b>23.72</b>	<b>34.49</b>	<u>36.21</u>	<b>32.55</b>	<b>15.43</b>	<u>20.67</u>	<b>20.20</b>	<u>24.24</u>	<b>66.50</b>	<b>87.37</b>	35.01	4.04	<b>11.50</b>	<u>49.90</u>	<b>50.89</b>	<b>33.17</b>
Llama3-70B-Instruct, $B_{\text{total}} = Full$																	
Full	27.75	46.48	49.68	52.04	54.90	30.44	32.37	22.20	27.62	73.50	92.46	45.72	12.00	72.50	41.70	69.06	46.90
Llama3-70B-Instruct, $B_{\text{total}} = 64L$																	
StreamingLLM	24.11	27.63	25.53	41.00	48.39	23.77	16.92	20.14	17.07	40.00	77.20	37.10	<u>12.00</u>	<b>72.50</b>	44.82	58.88	36.69
H2O	24.07	31.33	27.49	44.83	49.09	25.14	<b>22.31</b>	20.59	<b>24.30</b>	49.50	<b>91.45</b>	40.29	<u>12.00</u>	<b>72.50</b>	44.97	60.63	40.03
TOVA	<u>24.53</u>	30.43	27.56	45.29	49.64	25.93	<u>22.30</u>	20.08	<u>23.46</u>	48.66	<u>91.18</u>	40.23	11.85	<b>72.50</b>	44.31	60.65	39.91
SnapKV	23.97	<u>32.92</u>	<u>34.96</u>	<u>46.35</u>	<u>52.90</u>	<u>26.05</u>	18.33	<u>21.55</u>	19.98	43.00	88.83	<b>41.18</b>	<u>12.00</u>	<b>72.50</b>	44.42	<b>61.63</b>	<u>40.04</u>
ReST-KV	<b>26.32</b>	<b>36.38</b>	<b>38.44</b>	<b>49.51</b>	<b>53.18</b>	<b>26.20</b>	20.02	<b>21.81</b>	21.48	<b>59.75</b>	88.51	<u>40.51</u>	<b>12.05</b>	<u>71.50</u>	<b>45.22</b>	<u>61.22</u>	<b>42.01</b>
Llama3-70B-Instruct, $B_{\text{total}} = 512L$																	
StreamingLLM	24.62	31.89	31.23	44.91	47.51	25.91	23.08	19.76	24.15	62.50	88.14	43.36	<u>12.00</u>	<b>72.50</b>	<b>48.71</b>	66.04	41.64
H2O	27.56	42.91	36.19	50.40	49.87	25.98	<b>28.82</b>	21.67	<u>27.06</u>	72.00	91.88	44.57	<u>12.00</u>	<u>72.00</u>	42.65	67.87	44.59
TOVA	27.51	42.49	35.71	51.02	50.42	25.12	<u>27.88</u>	21.60	<b>27.28</b>	<u>72.04</u>	<u>92.04</u>	45.13	<b>12.89</b>	71.18	43.51	68.53	44.65
SnapKV	<u>27.67</u>	<u>44.58</u>	<u>48.00</u>	<b>51.66</b>	<u>53.73</u>	<b>30.61</b>	24.80	<b>22.82</b>	25.89	70.00	<b>92.63</b>	<u>45.14</u>	<u>12.00</u>	<b>72.50</b>	<u>44.59</u>	<b>69.20</b>	<u>45.99</u>
ReST-KV	<b>27.85</b>	<b>45.21</b>	<b>50.06</b>	<u>51.55</u>	<b>54.45</b>	<u>29.83</u>	25.77	<u>22.54</u>	25.83	<b>72.50</b>	<b>92.63</b>	<b>46.59</b>	<u>12.00</u>	<b>72.50</b>	43.44	<u>68.95</u>	<b>46.36</b>

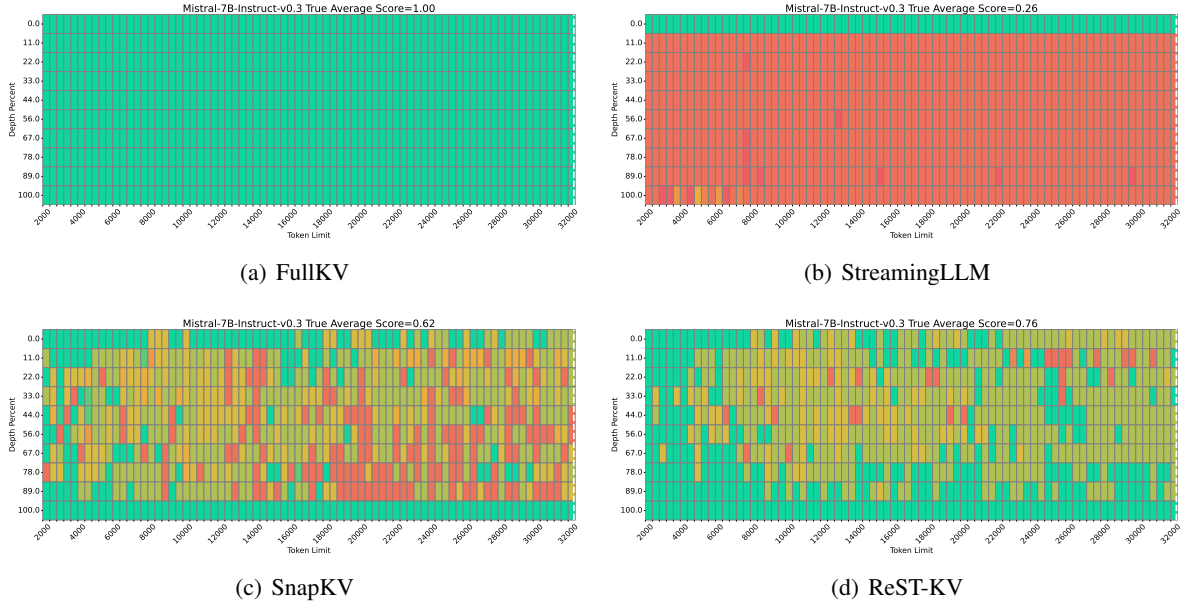


Figure 7: Performance comparison on the Needle in a Haystack Test using Mistral-7B-Instruct-v0.3 with  $B_{\text{total}} = 128L$ .

- **Llama3.1-8B-Instruct** ( $B = 1024L$ ) attains **100%** accuracy, meaning it can match full KV cache performance while storing only **1/32** of the original tokens. This highlights the efficiency of our approach in long-context retrieval with minimal memory usage.

Table 11: Performance comparison of ReST-KV and baseline eviction strategies on the RULER benchmark across multiple context lengths (4k to 128k tokens). Results are reported as average accuracy (%) over subtasks. ReST-KV consistently outperforms other methods, particularly on retrieval and multi-hop reasoning tasks. The best result is highlighted in **bold**, and the second-best is underlined.

Method	S-NIAH-1	S-NIAH-2	S-NIAH-3	MK-NIAH-1	MK-NIAH-2	MK-NIAH-3	MQ-NIAH	MV-NIAH	CWE	FWE	VT	Avg. Acc
Llama-3.1-8B-Instruct, $B_{\text{total}} = 1024L$ , context length=4k												
Full	100.0	100.0	99.60	100.0	100.0	99.60	99.90	96.25	99.78	97.67	99.96	99.34
StreamingLLM	27.8	30.6	<u>31.40</u>	34.2	26.2	29.6	28.7	30.05	73.2	<b>96.13</b>	30.0	39.81
SnapKV	<b>100.00</b>	99.0	20.6	99.6	93.0	<u>31.00</u>	99.2	90.45	<u>91.46</u>	95.33	<b>99.96</b>	<u>83.60</u>
PyramidKV	<b>100.00</b>	<u>99.80</u>	9.6	<b>100.00</b>	<u>96.80</u>	26.2	<u>99.70</u>	<u>93.60</u>	74.88	94.33	<u>99.92</u>	81.35
ReST-KV	<b>100.00</b>	<b>100.00</b>	<b>99.60</b>	<b>100.00</b>	<b>100.00</b>	<b>49.80</b>	<b>99.95</b>	<b>97.00</b>	<b>91.78</b>	<u>96.07</u>	99.92	<b>94.01</b>
Llama-3.1-8B-Instruct, $B_{\text{total}} = 1024L$ , context length=8k												
Full	100.0	100.0	100.0	100.0	99.80	98.80	100.0	95.75	97.62	95.27	99.92	98.83
StreamingLLM	11.0	12.0	<u>13.00</u>	14.2	11.0	<u>11.80</u>	12.35	12.45	4.36	86.93	13.56	18.42
SnapKV	<b>100.00</b>	98.4	12.0	98.0	85.6	7.6	97.8	87.45	<b>56.06</b>	88.27	<b>99.76</b>	<u>75.54</u>
PyramidKV	<b>100.00</b>	<u>99.80</u>	3.0	<u>99.20</u>	<u>87.80</u>	5.2	<u>98.05</u>	<u>88.25</u>	40.24	<u>89.00</u>	99.68	73.66
ReST-KV	<b>100.00</b>	<b>100.00</b>	<b>95.60</b>	<b>100.00</b>	<b>99.80</b>	<b>19.60</b>	<b>100.00</b>	<b>95.80</b>	<u>51.16</u>	<b>91.53</b>	<b>99.76</b>	<b>86.66</b>
Llama-3.1-8B-Instruct, $B_{\text{total}} = 1024L$ , context length=16k												
Full	100.0	100.0	100.0	99.60	100.0	99.00	99.85	98.25	90.90	96.67	99.80	98.55
StreamingLLM	5.6	6.4	<u>5.80</u>	7.2	6.0	<u>5.00</u>	5.2	6.7	0.18	78.53	6.52	12.1
SnapKV	<b>100.00</b>	97.0	4.0	97.8	74.0	3.8	<u>97.25</u>	<u>88.95</u>	<b>27.36</b>	92.6	99.6	<u>71.12</u>
PyramidKV	<b>100.00</b>	<u>97.40</u>	1.2	<u>98.00</u>	<u>75.20</u>	3.4	97.0	86.5	18.98	<u>95.07</u>	<b>99.80</b>	70.23
ReST-KV	<b>100.00</b>	<b>100.00</b>	<b>93.00</b>	<b>99.60</b>	<b>99.80</b>	<b>17.00</b>	<b>100.00</b>	<b>96.10</b>	<u>22.86</u>	<b>97.13</b>	<b>99.80</b>	<b>84.12</b>
Llama-3.1-8B-Instruct, $B_{\text{total}} = 1024L$ , context length=32k												
Full	100.0	100.0	100.0	100.0	100.0	99.60	99.90	98.95	48.60	97.07	99.68	94.89
StreamingLLM	3.6	1.8	2.4	3.0	3.8	<u>2.00</u>	2.5	2.45	0.12	<b>91.13</b>	3.52	10.57
SnapKV	<b>100.00</b>	<u>97.20</u>	<u>6.20</u>	<u>99.40</u>	<u>61.00</u>	2.0	96.5	<u>87.25</u>	<b>16.96</b>	71.27	<b>98.64</b>	<u>66.95</u>
PyramidKV	<b>100.00</b>	97.2	2.8	99.2	59.2	1.8	<u>96.55</u>	85.2	<u>10.52</u>	75.2	<u>98.60</u>	66.02
ReST-KV	<b>100.00</b>	<b>100.00</b>	<b>98.20</b>	<b>99.60</b>	<b>99.00</b>	<b>15.20</b>	<b>99.95</b>	<b>97.60</b>	9.36	<u>83.53</u>	98.16	<b>81.87</b>
Llama-3.1-8B-Instruct, $B_{\text{total}} = 1024L$ , context length=64k												
Full	100.0	100.0	99.80	99.80	99.20	94.00	99.75	98.95	7.96	90.60	98.32	89.85
StreamingLLM	2.0	1.6	2.4	2.6	2.0	<u>0.80</u>	2.05	2.8	0.14	<b>90.87</b>	1.76	9.91
SnapKV	<b>100.00</b>	96.4	<u>3.20</u>	99.00	32.2	0.2	91.7	<u>58.45</u>	<b>2.86</b>	54.53	93.60	57.47
PyramidKV	<b>100.00</b>	<u>96.80</u>	1.0	99.0	36.80	0.2	<u>92.10</u>	58.25	<u>1.66</u>	55.87	<b>94.56</b>	<u>57.84</u>
ReST-KV	<b>100.00</b>	<b>100.00</b>	<b>90.80</b>	<b>100.00</b>	<b>96.80</b>	<b>15.60</b>	<b>98.95</b>	<b>97.30</b>	1.3	<u>71.67</u>	92.68	<b>78.65</b>
Llama-3.1-8B-Instruct, $B_{\text{total}} = 1024L$ , context length=128k												
Full	97.40	97.80	95.20	96.20	87.00	63.20	95.85	94.95	0.06	64.73	80.08	79.32
StreamingLLM	0.4	2.0	<u>3.00</u>	2.4	0.6	<u>0.80</u>	1.95	2.35	<b>1.26</b>	<b>74.73</b>	0.52	8.18
SnapKV	<b>97.40</b>	<u>96.80</u>	1.4	93.8	25.6	0.0	80.6	27.0	0.08	30.47	<u>74.76</u>	47.99
PyramidKV	<b>97.40</b>	96.8	0.2	<u>94.20</u>	<u>30.80</u>	0.4	<u>80.95</u>	<u>29.20</u>	0.14	32.07	<b>76.08</b>	48.93
ReST-KV	<b>97.40</b>	<b>98.00</b>	<b>75.80</b>	<b>95.40</b>	<b>74.00</b>	<b>3.60</b>	<b>92.15</b>	<b>93.70</b>	<u>0.16</u>	<u>47.73</u>	73.12	<b>68.28</b>

These results further validate the robustness and efficiency of our method in selecting the most relevant KV pairs while minimizing memory overhead. Notably, even with a significantly reduced cache budget, our approach consistently outperforms prior methods, ensuring reliable long-context retrieval across different models and settings.

## G Additional Experiments on Ablation Study

In this section, we conduct additional ablation experiments to rigorously analyze the effectiveness of core components in ReST-KV and assess its sensitivity to key hyper-parameters.

### G.1 Efficacy of the Proposed Output Reconstruction Indicator

To evaluate the proposed eviction indicator, we compare it with different types of eviction indicators under the same baseline, including random selection, attention weights, attention weights weighted by the values’s norm ( $\mathbf{A}_t[n] \cdot \|\mathbf{v}_n\|_2$ ), similar to the VATP method (Guo et al., 2024), and our output reconstruction. As shown in Table 12, directly weighting attention weights by the values’s norm does not effectively incorporate the values information. Our method significantly outperforms all baselines, indicating that the layer-wise output reconstruction perspective better assesses the importance of KV cache.

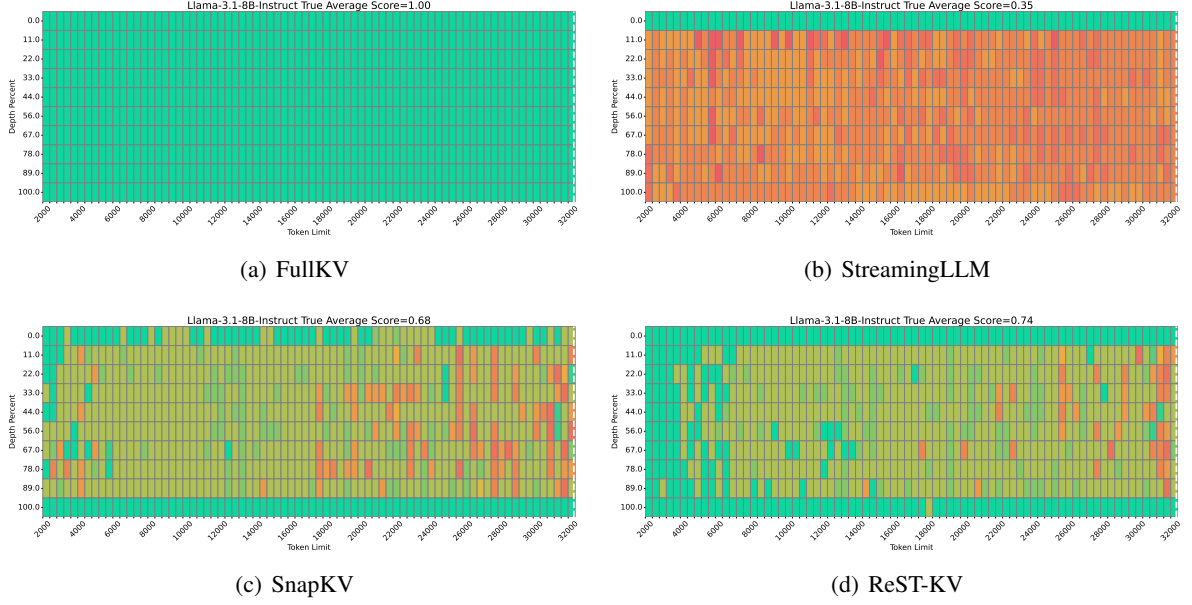


Figure 8: Performance comparison on the Needle in a Haystack Test using Llama3.1-8B-Instruct with  $B_{\text{total}} = 128L$ .

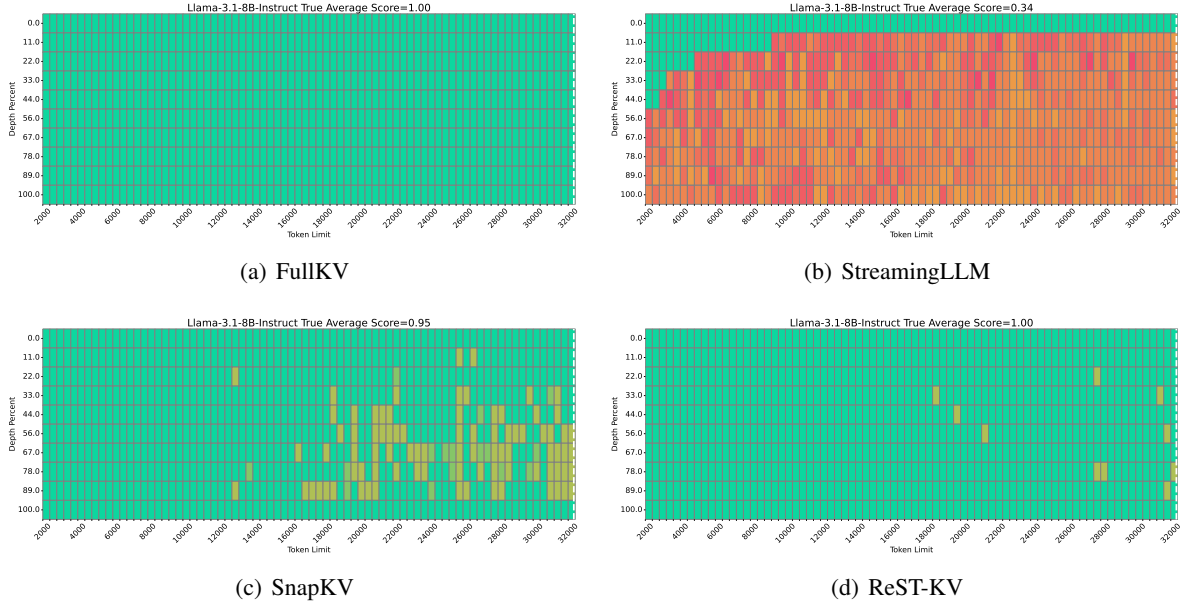


Figure 9: Performance comparison on the Needle in a Haystack Test using Llama3.1-8B-Instruct with  $B_{\text{total}} = 1024L$ .

Table 12: Ablation study on different types of information considered by the eviction indicator. Using output reconstruction as the eviction criterion achieves the best performance, surpassing methods based on attention weights or their combinations.

Information Considered by Eviction Indicator	Avg.
Random	$6.83 \pm 0.20$
Attention weights (SnapKV)	33.95
Attention weights and values (VATP)	33.88
Output reconstruction (Eq. (7))	<b>35.86</b>



## G.2 Efficacy of the Proposed Spatial-Temporal Smoothing

To assess the effectiveness of the spatial-temporal smoothing mechanism, we perform an ablation study to examine the impact of different smoothing methods. As shown in the left part of Table 13, various temporal smoothing techniques, including Mean, Inv-EMA, and EMA, are tested. Notably, EMA smoothing achieves the best performance, surpassing other baselines, which demonstrates its effectiveness in capturing temporal variations by giving higher weights to more recent KV pairs.

Table 13: Ablation study on the effect of different temporal and spatial smoothing methods in the eviction indicator. EMA refers to our proposed exponential moving average temporal smoothing, while AWS represents our adaptive window-based spatial smoothing.

Temporal Smoothing	Avg.	Spatial Smoothing	Avg.
None	35.22	None	33.50
Mean	34.02	Avgpool	35.69
Inv-EMA	31.25	Maxpool	35.59
EMA (Ours)	<b>35.86</b>	AWS (Ours)	<b>35.86</b>

In addition, we evaluate the spatial smoothing methods, as detailed in the right part of Table 13. Methods such as Avgpool, Maxpool, and our adaptive window-based smoothing (AWS) are compared, with AWS achieving the highest average performance. This suggests that the adaptive window-based approach, significantly enhances the eviction indicator’s ability to adjust for varying window sizes and offsets, thereby improving the assessment of the importance of KV pairs in the spatial-temporal context.

## G.3 Hyper-parameter Sensitivity Analysis

To assess the robustness of ReST-KV, we examine its sensitivity to two primary hyper-parameters: the temporal smoothing factor  $\alpha$  and the spatial smoothing scaling factor  $\beta$ .

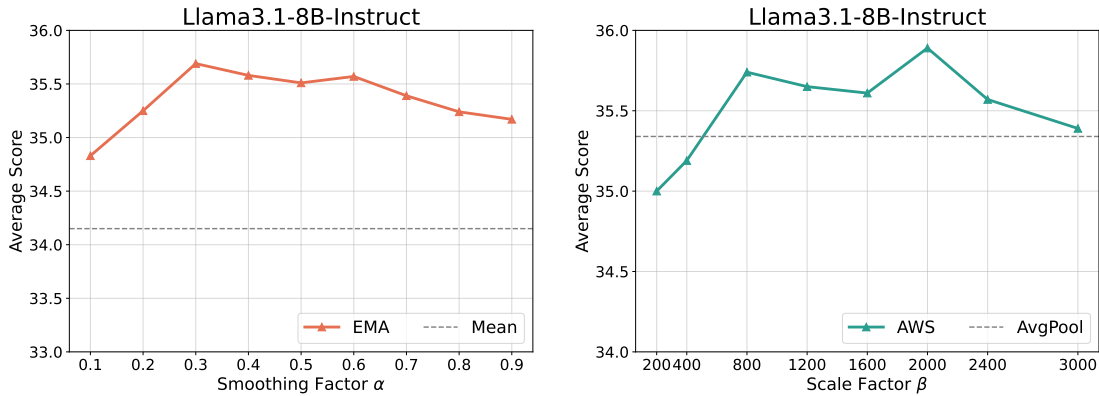


Figure 10: Sensitivity analysis of the smoothing factor  $\alpha$  (left) and scaling factor  $\beta$  (right). The performance remains relatively stable across different settings of both hyperparameters, mostly outperforming the baseline.

Figure 10 illustrates the performance variation with respect to  $\alpha$  (left panel) and  $\beta$  (right panel). The observed stability in accuracy across the tested ranges for both parameters indicates that ReST-KV exhibits low sensitivity to their specific values. This robustness offers considerable flexibility in hyper-parameter configuration without substantial performance degradation.

## H Additional Experiments on Efficiency

In this section, we investigate the integration of ReST-KV with prefill optimization techniques—exemplified by Minference (Jiang et al., 2024) and FlexPrefill to assess potential improvements in Time To First Token (TTFT). To this end, we conduct additional experiments on the RULER 128k

benchmark using the LLaMA3.1-8B-Instruct model, focusing on the efficiency of our proposed KV cache eviction method, particularly its impact on TTFT and decoding latency. Results are summarized in Table 14.

Table 14: Efficiency analysis on RULER 128k. All results are normalized to the Full KV caching baseline.

Method	128k Avg. Acc.	TTFT	Decoding Latency
Full	79.32	$1\times$	$1\times$
ReST-KV	68.28	$0.97\times$	$10.61\times$
ReST-KV+MInference	53.71	$2.99\times$	$10.41\times$
ReST-KV+FlexPrefill( $\gamma = 0.9$ )	67.16	$3.42\times$	$10.46\times$
ReST-KV+FlexPrefill( $\gamma = 0.95$ )	68.12	$2.37\times$	$10.54\times$

Our method is a KV cache eviction strategy that achieves a substantial improvement in decoding latency—over  $10\times$  speedup—while maintaining a comparable TTFT ( $0.97\times$ ) to full KV caching. Importantly, it maintains a high level of accuracy (68.28%), demonstrating that our eviction strategy preserves model performance effectively even under long context scenarios.

Furthermore, our method is orthogonal and compatible with sparse prefilling techniques such as MInference (Jiang et al., 2024) and FlexPrefill (Lai et al., 2025). When combined with these methods, we observe additional gains in TTFT. For example, integrating FlexPrefill with  $\gamma = 0.95$  achieves a  $2.37\times$  TTFT speedup while retaining high decoding efficiency ( $10.54\times$  latency speedup) and competitive accuracy (68.12%). This shows that our approach not only accelerates decoding but also enables efficient and flexible integration with other prefill optimization techniques.

## I Integration with KV Cache Quantization

In this section, we further investigate the interplay between ReST-KV and established KV cache quantization techniques, specifically KIVI (Liu et al., 2024b) and KVQuant (Hooper et al., 2024). Our goal is to evaluate whether combining ReST-KV—a KV eviction method that accounts for the effects of attention redistribution and the spatial-temporal dynamics in KV selection can synergize with quantization or even outperform aggressive quantization applied to a full, non-evicted KV cache under similar overall compression ratios.

To this end, we compare ReST-KV, both in isolation and combined with KIVI and KVQuant, against a baseline using full KV cache with various bit-width quantizations. Figure 11 visually summarizes the results.

In particular, even with a stringent total compression ratio of 6.25%, achieved by combining ReST-KV with moderate 4-bit quantization, ReST-KV retains high average accuracy. In contrast, applying more aggressive 2-bit KIVI or KVQuant directly to the full KV cache results in significantly lower accuracy.

These results suggest that eviction strategies which explicitly account for attention redistribution and spatial-temporal token redundancy can provide a more effective pathway to KV cache compression than quantization-only approaches. The combination of ReST-KV and lightweight quantization thus offers a practical and robust solution for efficient inference under tight memory constraints.

## J Additional Experiments on InfiniteBench

In this section, we evaluate ReST-KV on the InfiniteBench benchmark (Zhang et al., 2024b) to further assess its long-context capabilities. InfiniteBench tests LLM performance on extremely long sequences through a diverse set of tasks. These tasks include realistic scenarios such as novel-based reasoning (summarization, QA, multiple-choice, using novels with key entity replacement), dialogue understanding, and code debugging. Additionally, synthetic tests probe specific long-context abilities like retrieval, state preservation, and sequential processing.

Experiments are conducted on the Llama3.1 model. We compare ReST-KV against SnapKV (Li et al., 2024b), as both are post-prefill KV eviction strategies. To ensure a direct comparison of their eviction

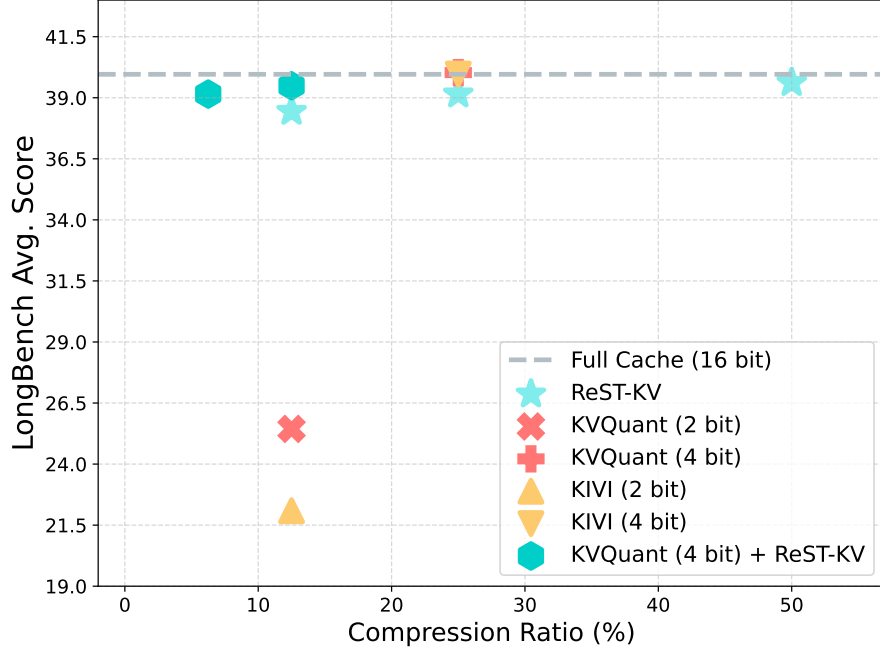


Figure 11: Comparison of ReST-KV, KV cache quantization methods (KIVI and KVQuant), and their combination on Llama3.1-8B-Instruct using LongBench dataset.

effectiveness, both methods retain a fixed KV cache budget of 1024 tokens post-eviction, regardless of the initial input context length.

Table 15 details the average performance across InfiniteBench subtasks. ReST-KV achieves a notably higher overall average accuracy than SnapKV (e.g., 38.8% vs. 36.8%). This performance advantage is particularly evident in retrieval-focused tasks (Retrieve.PassKey, Retrieve.Number, Retrieve.KV), where SnapKV can exhibit critical failures on some subtasks. ReST-KV also generally demonstrates stronger results in question answering (En.QA, Zh.QA) and Math.Find. While SnapKV may be competitive on select tasks like En.Sum, the consistent and superior performance of ReST-KV across a wider range of demanding retrieval and reasoning tasks contributes to its substantially higher overall average. These findings underscore the efficacy of ReST-KV’s reconstruction-aware eviction strategy when applied to the challenging long-context scenarios presented by InfiniteBench.

Table 15: Performance of different methods on InfiniteBench.

Methods	Retr.PassKey	Retr.Num	Retr.KV	En.Dia	En.Sum	En.MC	En.QA	Zh.QA	Math.Find	Debug	Avg.
ReST-KV	<b>100.0</b>	<b>93.7</b>	<b>11.4</b>	<b>10.5</b>	22.9	67.2	<b>13.2</b>	<b>13.1</b>	<b>34.0</b>	<b>22.3</b>	<b>38.8</b>
SnapKV	<b>100.0</b>	87.1	0.0	10.0	<b>23.7</b>	<b>67.7</b>	11.3	12.2	<b>34.0</b>	<b>22.3</b>	36.8